Biogeotechnics 1 (2023) 100008

Contents lists available at ScienceDirect

Biogeotechnics

journal homepage: www.keaipublishing.com/en/journals/biogeotechnics/

Applications of microbial-induced carbonate precipitation: A state-of-the-art review

Yuze Wang[a,*], Charalampos Konstantinou[b], Sikai Tang[a], Hongyu Chen[a]

[a] Department of Ocean Science and Engineering, Southern University of Science and Technology, Shenzhen 518055, China
[b] Department of Civil and Environmental Engineering, University of Cyprus, Nicosia 2109, Cyprus

ARTICLE INFO

Keywords:
MICP
Mechanisms
Engineering properties
Engineering applications

ABSTRACT

Microbial-Induced Carbonate Precipitation (MICP) is a naturally occurring process whereby bacteria produce enzymes that accelerate the precipitation of calcium carbonate. This process is facilitated through various bacterial activities, including ureolysis, sulfate reduction, iron reduction, and denitrification. The application of MICP has been widespread in a range of engineering fields, such as geotechnical, concrete, environmental, and oil and gas engineering for soil stabilization, concrete remediation, heavy metal solidification, and permeability control. Numerous review papers have been published that summarize the mechanisms and properties associated with different MICP applications. The purpose of this review paper is to provide a comprehensive summary of the various engineering applications of MICP, along with the mechanisms, materials, and engineering properties associated with each application. By comparing the similarities and differences in MICP research progress across different engineering fields, this review aims to increase understanding of MICP, stimulate new research ideas, and accelerate the development of MICP techniques.

1. Introduction

Microbial-induced carbonate precipitation (MICP) is a natural process where bacterial activity alters the aqueous medium's supersaturation conditions, resulting in the precipitation of carbonate minerals. Compared to the naturally occurring process of carbonate mineralization, MICP occurs more rapidly due to the action of bacterial enzymes. There are several pathways by which microbial metabolism activity increases the pH of the aqueous medium, promoting MICP. These pathways include ureolysis, sulfate reduction, iron reduction, and denitrification etc.

The precipitated calcium carbonate crystals can bind soil particles together, increasing soil strength and stiffness while controlling for relatively high permeability. Compared to cement, the viscosity of the bacterial suspension is low, making it possible to inject into small pores or cracks in the structure so that the precipitated crystals can fill the small cracks. Carbonate precipitates can also change the surface properties of oil-water separation materials, improving separation efficiency. Additionally, carbonate minerals can co-precipitate with heavy metals, increasing the solidification of contaminated soils. Carbonate precipitation is also an effective carbon sequestration method, making MICP widely applicable in geotechnical, environmental engineering, hydraulics, groundwater ecohydrology, oil and gas industry, engineering geology, ocean engineering, structural engineering, and other fields.

MICP mechanisms and engineering properties have been extensively studied experimentally at different scales, from microscale using scanning electron microscopy, microfluidics, and micro-CT, to core scale using cube experiments combined with a series of mechanical testing methods, and to large-scale laboratory and field experiments with *in situ* monitoring methods. Factors affecting the success and performance of MICP include MICP protocols, such as bacterial, chemical, and injection properties, solid medium properties, such as porosity, pore structure, etc., and environmental factors, such as temperature, oxygen level, aqueous medium salt content, pressure, and local bacterial communities.

This review provides an overview of the various applications of MICP and factors that impact its properties. Additionally, it identifies research gaps, challenges, and future directions for the use of MICP in different applications.

* Corresponding author.
E-mail addresses: wangyz@sustech.edu.cn (Y. Wang), ckonst06@ucy.ac.cy (C. Konstantinou).

https://doi.org/10.1016/j.bgtech.2023.100008
Received 15 February 2023; Received in revised form 1 March 2023; Accepted 10 March 2023
Available online 27 March 2023

2. Filling fractures or pores of geoformations for underground projects

In 1992, Ferris and Stehmeier [30] introduced the application of MICP for hydraulic control of geoformations by publishing a U.S. Patent titled "Bacteriogenic mineral plugging" (U.S. Patent 5143,155, September 1, 1992). This marked the beginning of using MICP for various applications such as (i) well closure, (ii) manipulating subsurface flow paths to enhance oil recovery, (iii) sealing ponds or reservoirs, (iv) forming subsurface barriers to control saltwater or contaminated groundwater intrusion, and (v) treating fractures in cap rocks, wellbore cements, or casing/cement/formation interfaces to mitigate leakage from geologically sequestered CO_2 injection sites. These applications require a significant reduction in the permeability of fractured geoformations or hydraulic conductivity of the porous medium. This section presents recent trends and research conducted on these applications. Table 1 provides a summary of MICP research conducted on filling fractures or pores of geoformations in underground projects, and Fig. 1(a) illustrates these findings.

2.1. Sealing ponds, plugging reservoirs and landfill barriers

Applications such as sealing ponds, plugging reservoirs, and building landfill barriers require a reduction in the permeability of granular materials with pores, such as soils and porous sandstone. To achieve this, several studies have utilized microbial-induced carbonate precipitation (MICP). For instance, Chu et al. [19] reported a reduction in sand permeability from 10^4 m/s to 10^7 m/s with an average of 2.1 kg of calcium (Ca) per m^3 precipitated on sand particles. Stabnikov et al. [111] utilized ferric hydroxide precipitation, produced by a ferrous-containing solution percolated from iron ore and cellulose, along with a combination of acidogenic and iron-reducing bacteria, to reduce sand hydraulic conductivity from 10^{-4} m/s to 10^{-8} m/s. Zhong et al. [146] demonstrated an 88.6% reduction in permeability from 1500 milli darcies (md) to 136 md in a high-permeability reservoir and a decrease to 22 md in a low-permeability reservoir. MICP treatment also led to a 7.9% increase in reservoir recovery. Furthermore, Hataf and Baharifard [42] showed that MICP-treated soil samples experienced decreased permeability, suggesting that MICP could be a useful and environmentally friendly method to form a barrier between waste and groundwater or substrata.

2.2. Wellbore integrity and fracture sealing

MICP can reduce permeability in formations with carbonate precipitation, which is relevant for applications such as wellbore integrity and fracture sealing. Several studies have demonstrated the effectiveness of MICP in reducing permeability and improving wellbore integrity. Cuthbert et al. [23] conducted a field-scale experiment that significantly reduced the permeability of a single fracture over several square meters. Cunningham et al. [22] showed that MICP reduced the permeability of a Berea sandstone core by more than 3 orders of magnitude and improved wellbore integrity. In another study, Phillips et al. [95] successfully treated compromised wellbore cement using MICP. Tobler et al. [117] applied MICP to treat fractured granite cores, and Wu et al. [127] performed 3D scanning and simulation on MICP-treated fractured rock. Kirkland et al. [57] utilized MICP for wellbore integrity applications and suggested that it can be employed to remediate leakage pathways and improve waterflood efficiency. Peng et al. [94] showed that MICP grouting can significantly reduce the permeability of fractured rock. Lastly, Kolawole et al. [58] suggested that MICP can enhance the long-term caprock integrity and CO_2 storage security.

3. Binding granular materials whilst maintaining drainage ability

MICP can enhance soil strength and stiffness by binding soil particles with precipitated calcium carbonate crystals without filling soil pores completely. This results in improved drainage ability while adding a controlled amount of cementation within the granular network. This process has a variety of applications, including stabilization of onshore and offshore soils, liquefaction provision, dust and desertification control, and erosion control. Table 2 summarizes research on MICP for binding granular materials while maintaining drainage ability, and Fig. 1(b) provides an illustration of the process.

3.1. Stabilization of onshore and offshore soils

The ability of $CaCO_3$ crystals produced by MICP to bind soil particles and maintain soil permeability is directly influenced by properties such as crystal type, size, number, and distribution. These properties can be analyzed using scanning electron microscopy (SEM), which has been used by researchers to understand the mechanisms of increased soil strength through MICP treatment. For instance, studies have shown that precipitated calcite can form bonds at particle-particle contacts [27], lower chemical concentrations of $CaCO_3$ lead to better distribution of calcite precipitation [2] and that larger rhombohedral $CaCO_3$ crystals precipitate around the bio-slurry of spherical fine crystals [12]. In addition, Mahawish et al. [79] observed both large calcium carbonate crystals and microbes. While SEM is useful, it cannot capture the entire MICP process. To overcome this, microfluidic chips have been designed and fabricated to observe the spatial and temporal changes in $CaCO_3$ crystal properties during MICP treatment. In previous studies, Wang et al. [123,121] utilized scanned photos of sandy soil to design and produce microfluidic chips. The channel inside the chips were made hydrophilic and MICP treatment procedures were performed. It was discovered that the properties of $CaCO_3$ crystals may vary both spatially and temporally [120]. Changes in bacterial quantity during MICP treatment can be measured [121], and the effects of bacterial density and temperature on crystal growth rate and transformation processes were explored ([122]). The time interval between injections of cementation solution was identified to affect the number and size of crystals produced following MICP treatment in accordance with Ostwald's law [120]. This discovery was applied to a soil column experiment which demonstrated that longer intervals between injections resulted in larger $CaCO_3$ crystals and thus were more effective in enhancing the strength of MICP-treated sand. By using Raman backscattering spectroscopy to analyze the chemical composition of the precipitate, Xiao et al. [132] identified calcite and vaterite as the main mineral phases in microfluidic chips. Furthermore, Xiao et al. [131] discovered that high concentrations of calcium chloride ($CaCl_2$) hindered diffusion and decreased the uniform distribution of $CaCO_3$ at the microscale. In another study, Marzin et al. [82] placed grains in a microfluidic cell and discovered that NaCl in solution increased the adhesion rate of bacteria.

In order to stabilize soil, it is important to increase its strength and stiffness. To achieve this, the stress-strain behavior of microbial-induced calcium carbonate precipitation (MICP) has been investigated. According to DeJong et al. [27], MICP-treated specimens exhibit non-collapse strain softening shear behavior, with higher initial shear stiffness and ultimate shear capacity compared to untreated loose specimens. Montoya & DeJong [84] found that the peak strength of MICP-treated soils generally increases with the $CaCO_3$ content, and the soil's behavior transitions from strain-hardening to strain-softening. Montoya and DeJong [84] measured s-waves using bending elements and showed that the small-strain shear stiffness (G_{max}) of MICP-treated samples was 634 MPa, 1815 MPa and 2940 MPa when the $CaCO_3$ content was 1.3%, 3.06% and 5.31%, respectively.

Table 1
Filling fractures or pores of geoformations for underground projects.

References	Application	Bacterial Strain	Cementation solution	Treating material	Testing
Sealing ponds, plugging reservoirs and landfill barriers					
[19]	construction of an aquaculture pond	*Bacillus sp. VS1*	0.75 M $CaCl_2$ and 1.5 M urea	Ottawa sand with a mean grain size of 0.42 mm	field emission scanning electron microscope (FE-SEM); water leakage tests; permeability tests; four-point bending tests; unconfined compression (UC)
[111]	construction of an aquaculture pond	*urease-active bacteria, acidogenic and iron-reducing bacteria*	$CaCl_2$ and urea	standard sand ASTM C778	Falling head permeability tests; X-ray-diffraction (XRD)
[146]	enhanced oil recovery	*Bacillus subtilis*	glucose and urea	quartz sand	permeability and porosity Measurements; Oil repelling experiment
[42]	Barrier	*B. sphaericus*	20 g/l urea 100 g/l $CaCl_2$	Shiraz landfill base soil	Falling head permeability tests
Pollution mitigation, Wellbore integrity and fracture sealing					
[23]	Pollution mitigation	*S.pasteurii*	0.4 M urea	fractured subsurface rock	MICP field experiment
[22]	Wellbore leakage mitigation	*Sporosarcina pasteurii*	Nutrient sources; urea; $CaCl_2$	fractured sandstone samples and formation	sandstone core experiments, meso-scale experiments and a field experiment
[96]	sealing subsurface fractures in the near wellbore environment	*Sporosarcina pasteurii*	99 g/L $CaCl_2$, 23.3 g/L NH_4Cl, 56 g/L urea, and 7.0 g/L mixed with brine	Sandstone Formation 340.8 m below ground surface	XRD, X-ray Micro Computed Tomography (Micro-CT)
[95]	wellbore cement integrity	*Sporosarcina pasteurii*	overnight grown inoculum amended with 5 g/L YE 24 g/L urea)	wellbore cement at a 310.0–310.57 m below ground surface	MICP field experiment, pressure-flow test, Mechanical integrity tests, ultrasonic imaging
[117]	hydraulic barrier	*S. pasteurii*		fractured granite cores	Micro-CT, Shear strength tests
[57]	remediate leakage pathways	*Sporosarcina pasteurii*	125 g/L $CaCl_2$ * 2 H_2O 72 g/L urea, 3 g/L NH_4Cl and 9 g/L yeast extract	tight oil-bearing sandstone	field application, XRD, FE-SEM
[127]	Permeability reduction	*Sporosarcina pasteurii*	bacteria culture and cementation solution	rock fractures with various initial apertures	3D scanning and 3D flow simulation
[94]	Permeability reduction	*S. pasteurii*	urea and calcium chloride	sandstone samples	SEM, energy dispersive spectrometer (EDS), permeability tests
[58]	enhance caprock integrity for CO_2 storage	*Sporosarcina pasteurii*	2.5 M urea and 2.5 M $CaCl_2$	shale samples with pre-existing fractures	UCS, complex transient method for permeability and Porosity Measurements, XRD, SEM

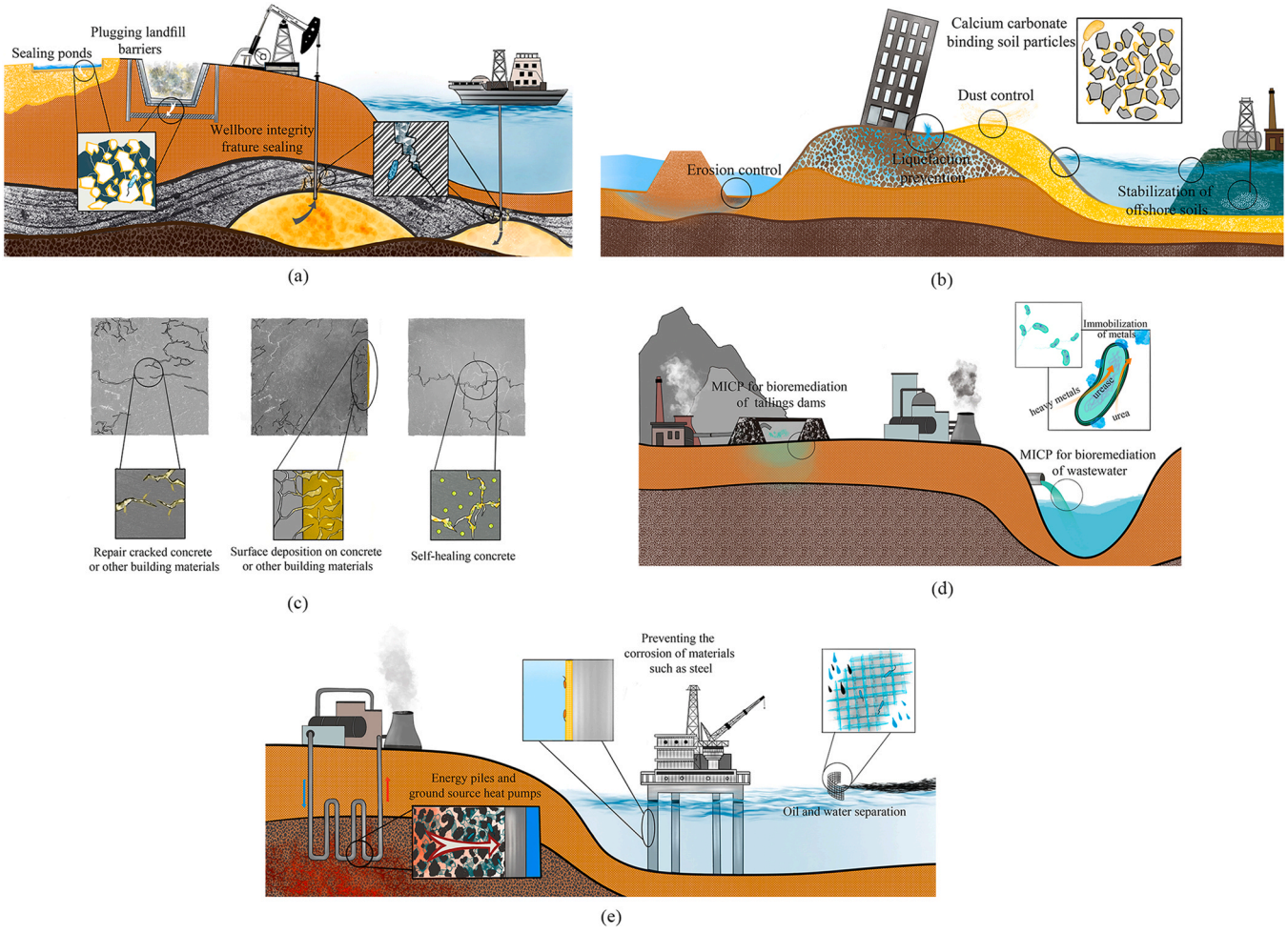

Fig. 1. Summary of MICP applications. (a) filling fractures or pores of geoformations in underground projects; (b) binding granular materials whilst maintaining drainage ability; (c) construction remediation; (d) bioremediation purposes; (e) material modification and protection.

Wu et al. [128] explained the stress-dilatancy relationship of bio-cemented sand using Rowe's stress-dilation theory, showing that bio-cemented sand behaves like dense sand in terms of stress-dilation relationship, and the higher the $CaCO_3$ content, the greater the expansion. The strength and stiffness behavior are highly affected by $CaCO_3$ content. Soon et al. [110] suggested that a minimum calcite content of 1.0% is required to provide measurable improvement in soil strength. Similarly, Lin et al. [73] showed that soil strength increased even when the calcium carbonate content was as low as 1%. Gao et al. [34] showed that a calcite content of 1.0% and 0.79% was sufficient to achieve shear strength in loose sand (Dr = 30%) and medium dense sand (Dr = 50%), respectively. Cui et al. [20] found that the effective friction angle (u_0) and the effective cohesion (c_0) increase with $CaCO_3$ content, and can be well-fitted using linear and exponential functions, respectively. Mahawish et al. [79] achieved a maximum compressive strength of around 14 MPa. Furthermore, at similar $CaCO_3$ content, the strength behavior may vary due to different MICP protocols producing $CaCO_3$ crystals with different microscale properties. Al Qabany & Soga [97] found that a lower chemical concentration resulted in stronger samples. Cheng et al. [13] found that higher soil strength can be obtained at a similar $CaCO_3$ content when the treatment is performed under a low degree of saturation.

In addition to increasing soil strength and stiffness, controlling hydraulic conductivity is also crucial for certain applications, whether it is necessary to maintain good drainage or to substantially reduce permeability. The amount and properties of $CaCO_3$ produced can alter the hydraulic properties of soil, with crystal amount and characteristics being determined by bio-chemical parameters, injection method, and porous medium characteristics. Achieving a balance of slower reactions can result in lower urease activities and chemical solution concentrations, which can lead to a lower reduction in hydraulic conductivity but still provide effective strength enhancement. However, for a complete reduction of permeability, high urease activities, flow rates, and chemical solution concentrations are required to plug the pores. Whiffin et al. [126] observed reductions in permeability ranging from 80% to 40% after treatment with varying post-treatment permeability values. Treatment recipes can also affect the size of the precipitated $CaCO_3$ crystals and thus the permeability. Al Qabany and Soga [97] found that high concentrations of urea and calcium chloride solutions caused a rapid drop in permeability during early stages of $CaCO_3$ precipitation, while a low-chemical-concentration solution resulted in a more gradual and uniform decrease in permeability. Al Qabany and Soga [97] showed that there was a greater reduction in permeability for samples with lower initial relative density, and Rowshanbakht et al. [101] found that the permeability of soil samples decreased as the relative density of soil increased. Mujah et al. [88] compared the strength and permeability of bio-cemented samples to those treated with ordinary Portland cement (OPC) and found that bio-cemented sand samples provided higher strength and permeability compared to samples treated with a similar content of OPC after 28 days of curing.

In the context of soil stabilization, achieving treatment homogeneity is of utmost importance. van Paassen et al. [91] conducted a large-scale study on biogrouting as a ground improvement method and demonstrated that seismic measurements can be utilized to monitor the

Table 2
Binding granular materials whilst maintaining drainage ability.

References	Application	Bacterial Strain	Cementation solution	Treating material	Testing
Soil stabilization					
[27]	undrained shear response of MICP-treated soil	*Bacillus pasteurii*	urea -$CaCl_2$ (140 g / L)	Ottawa 50–70 Sand	undrained compression, shear wave velocity, triaxial testing (CIUC), SEM, X-ray
[126]	MICP as a Soil Improvement Technique	*Sporosarcina pasteurii*	1.1 M Urea and $CaCl_2$	125–250 μm Itterbeck sand	5-meter-long column tests, Urease Activity, Ammonium Concentration, Calcium Concentration, Calcium Carbonate Content, Water Pressure, Strength, Stiffness, Porosity, and Permeability
[91]	Large-Scale Experiment Monitoring	*Sporosarcina pasteurii*	$CaCl_2$and urea 1 mol/L	poorly-graded, fine to medium grained	Large-Scale Experiment; Geophysical seismic measurements, UCS, shear-wave velocity, Monitoring
[2]; [97]	Transform efficiency	*S. pasteurii*;	0.1, 0.25, 0.5 and 1 M urea and calcium chloride	Fine and very fine sand	UCS, $CaCO_3$ content, Chemical efficiency, SEM
[81]	Optimization of MICP	*S. pasteurii*	3:3:1 (333 mM), 1:1:1 (50 mM)	Ottawa 50–70 and 20–30 silica sands	half-meter-scale column, shear wave velocity, permeability, calcium carbonate content, aqueous calcium, ammonium, urea, and bacterial density
[10,13]; [14], [15,12]	Bio-cementation at various degrees of saturation, one-phase low-pH injection method	*S. pasteurii*	1 M urea calcium chloride; artificial seawater	poorly graded sand	1-m sand column, Triaxial compression tests, SEM, permeability tests, Durability tests, UCS, EDX, XRD
[110]	Improvement in engineering properties of residual soil	*B. megaterium*	varying concentrations, and 3 g/L of nutrient broth	tropical residual soil	hydraulic conductivity, carbonate content, UCS, ammonium concentration, pH
[84]	Stress-strain behavior of Sands	*S. pasteurii*	333 mM urea, 374 mM NH_4Cl, 0–25.2 mM $NaHCO_3$, 0–3 g/L NB, 50 mM $CaCl_2$	Silica sand	Undrained Triaxial Compression, shear wave velocity
[73]	Mechanical Behavior of Sands	*S. pasteurii*	0.1 and 0.3 M	Ottawa 50–70 and 20–30 silica sands	Triaxial and confined compression tests, SEM, EDS, uniformity
[101]	Soil stabilization	*S. pasteurii*	1 M equimolar $CaCl_2$ and urea	Sand three RDs (40%, 70%, and 85%).	Ammonium concentration, UCS, Permeability, SEM
[20]; [21]	strength behaviour of bio-cemented sand	*S. pasteurii*	0.5, 1.0 M urea -$CaCl_2$	CHINA ISO standard sand; calcareous sand samples	Carbonate content, SEM, triaxial compression tests
[35]	Large-Scale Comparison of Bioaugmentation and Biostimulation Approaches	*S. pasteurii*	12.5 mM Ammonium chloride, 42.5 mM Sodium acetate, 350 mM urea, 0.1 g/L urea	Concrete sand, Monterey 12–20 sand, Yolo loam	1.7-m-diameter soil tank specimens, shear wave velocity, biogeochemical changes, cone penetration tests
[138]	Undrained Monotonic Shear Response	*Sporosarcina pasteurii*	50 mM $CaCl_2$ dehydrate, 374 mM NH_4Cl, 333 mM urea	Nevada sand, silica flour	Direct simple shear, SEM, EDS
[78]	Costal erosion control	*Sporosarcina pasteurii*	1 mol/L calcium chloride and 1 mol/L urea.	Calcareous sand from the Xisha Islands in the South China Sea.	UCS, splitting tensile tests, triaxial compression tests, SEM, XRD
[70]	Impact of oxygen availability on MICP	*Sporosarcina pasteurii*	molar ratio of urea and Ca^{2+} was 1:1	Standard sand from Xiamen, China	Bacterial biomass, dissolved oxygen, OCR, BUHR, UCS
[115]	3-D micro-architecture of MICP-treated sand	*Sporosarcina pasteurii*	-	sand	micro-CT scans, photomicroscopy, SEM, UCS
[69]	Ammonium By-product Removal for Ureolytic Bio-cementation	*Sporosarcina pasteurii*	250 mM calcium chloride and urea	Concrete sand, delta sand, Covelo sand	Shear wave velocity, ammonium measurements, pH
[79]	Strength and microstructure of bio-treated coarse sand	*S. pasteurii*	1 M urea and 1 M calcium chloride ($CaCl_2$)	Coarse sand (average grain size of 1.6 mm)	UCS, carbonate content, final porosity, MicroCT scanning, SEM imaging
[121,120,122]	MICP mechanisms, application of microfluidic chip for MICP	*Sporosarcina pasteurii*	mainly contains 0·25 M $CaCl_2{\cdot}2H_2O$), 0·375 M urea and 3 g/l nutrient broth	Microfluidic chip, silica sand	microscope image analysis, UCS, SEM
[130,132] [131]	Temperature-Controlled Method, Kinetic biomineralization	*Sporosarcina pasteurii (strain DSM 33)*	0.5 M urea and 0.5 M calcium chloride	Silica sand; Microfluidic chip	Drained triaxial tests, microscope image analysis
[127,128]	Large scale model tests, Stress-Dilatancy Behavior	*Sporosarcina pasteurii; Bacillus sp*	0.75 M urea and $CaCl_2$	Sand and rock	UCS, carbonate content, permeability, Triaxial consolidated drained (CD) tests, SEM
[88]	Optimisation of MICP process	*Bacillus sp.*	three final CS concentrations (0.25 M, 0.5 M, and 1 M)	sand	UCS, SEM, chemical efficiency

(*continued on next page*)

Table 2 (*continued*)

References	Application	Bacterial Strain	Cementation solution	Treating material	Testing
[34]	Mechanical behaviour of biocemented sands at various treatment levels and relative densities	*Sporosarcina pasteurii*	0.5 mol/L urea and 0.5 mol/L calcium chloride.	Ottawa sand, loose and medium dense sands	Triaxial CD tests and K0 consolidation tests, SEM
[93]	Influence of temperature on MICP	*Sporosarcina pasteurii*	Urea and the $CaCl_2$ in this study was set as 1.0 M and 0.5 M, respectively.	Ottawa silica sand	UCS, XRD, SEM, ureaolytic activity, carbonate contents
[82]	Adsorption Rate of Sporosarcina pasteurii Bacteria on Sandstone	*Sporosarcina pasteurii*	1.4 mol/L urea and $CaCl_2$ 155 g/L	Microfluidic chip	microscope image analysis
[116]	Full-Scale Application of Slope Stabilization	*Sporosarcina pasteurii*	40 mM calcium chloride and 50 mM urea	Field soil	SEM, GIS surveillance
[103]	Examining Spatial Control, Ammonium By-Product Removal	*Sporosarcina pasteurii*	250 mM urea and calcium chloride	poorly graded alluvial and marine sands	Meter-Scale Biocementation Experiments
[61]	Strength enhancement of soil for underground structures	*Sporosarcina pasteurii*	0.375 M of urea, 0.25 M of calcium chloride ($CaCl_2$), and 3 g/L of nutrient broth	Fine silica sand	
[136]	Seawater based MICP cements	*Sporosarcina pasteurii*	1 mol of urea and 1 mol of calcium chloride in 1 L of seawater	Loose sand blocks	Urease activity, Compressive Strength, SEM, XRD, Porosity
Liquefaction provision					
[85]	Dynamic response of liquefiable bio-treated sand	*Sporosarcina pasteurii*	1 M urea, 0.5 M calcium chloride	Ottawa 50–70 sand	Cyclic direct simple shear test, shear wave velocity
[43]	Undrained Responses of Microbially Desaturated Sand under Monotonic Loading	*Acidovorax sp.*		Ottawa sand	undrained triaxial compression and extension tests
[129]	Liquefaction resistance of bio-cemented calcareous sand	*Sporosarcina pasteurii*	0.5 mol/L urea and 0.5 mol/L $CaCl_2$.	calcareous sands were sourced from South China Sea.	Undrained cyclic triaxial (UCT) tests, SEM
[24]	Centrifuge Model Testing of Liquefaction Mitigation via MICP	*Sporosarcina pasteurii*	$CaCl_2$ (250 mM), Urea (350 mM)	Ottawa F-65 sand	Centrifuge testing, shear wave velocity, settlement, cone penetration resistance, maximum shear strain
[139]; [140]	Undrained cyclic response of MICP-treated silty sands; in situ delivery of MICP	*S. pasteurii*	50 mM $CaCl_2$ dehydrate, 374 mM NH_4Cl, 333 mM urea	Nevada sand, a fine grain silica sand, and non-plastic silt	Cyclic direct simple shear testing, shear wave velocity, Shear wave velocity, hydraulic conductivity, SEM, numerical modelling
[112]	Liquefaction Resistance of Biocemented Loess Soil	*S. pasteurii*	1.0 M of urea and 0.75 M of calcium acetate	Loess soil from the Loess Plateau area, Ningxia Hui Autono- mous Region, China	MICP solidification tests and undrained cyclic triaxial tests, Permeability, SEM
[105]	Large-scale spatial characterization and liquefaction resistance	*S. pasteurii and B. sphaericus*	0.50 M urea and cementation solution	Narmada River sand	Dynamic cone penetration, EC, TDS, and pH, SEM
[55]	Mechanical behaviour of MICP-treated silty sand	*S. pasteurii*	urea (0.3 M) and $CaCl_2$ (0.3 M).	Firoozkooh No. 161 silica sand and non-plastic Firoozkooh silica flour (silt)	Shear wave velocity, UCS, static and dynamic triaxial shear tests, SEM
Dust and deserfication control					
[36]	erosion resistance and dust control and future re-vegetation	*Sporoscarcina pasteurii*	the molar ratio of urea to calcium chloride remained at 2:1	a mine site location in the province of Saskatchewan, Canada	MICP field experiment, dynamic cone penetration (DCP) testing
[106]	the prevention of mine dust	*Bacillus pasteurii*	$CaCl_2$ and urea as raw materials	coal	SEM and EDS, XRD, wind resistance test
[147]	mitigate wind erosion	*Sporosarcina pasteurii*	nutrient broth (3 $g{\cdot}l^{-1}$), ammonium chloride (10 $g{\cdot}l^{-1}$) and sodium bicarbonate (2.12 $g{\cdot}l^{-1}$) prepared at 0.5 M concentration	angular to sub-angular medium silica sands, carbonate silty sand	wind tunnel experiments, mini-scale outdoor experiments, shear strength measurements
[71]	desertification control	*Sporosarcina pasteurii*	$NaHCO_3$ 2.12 g/L, nutrient broth 3 g/L, NH_4Cl 10 g/L, urea 30 g/L, $CaCl_2{\cdot}2\,H_2O$ 73.5 g/L. 0.5 mol/L of Ca^{2+}	Ulan Buh Desert, China	field test
[83]	reducing wind erosion of desert soil	*Sporosarcina pasteurii (ATCC 11859)*	0.1–1 M urea- $CaCl_2$	Ulan Buh Desert, Ningxia Hui Autonomous Region, China	Scanning electron microscopy (SEM), Field tests

(*continued on next page*)

Table 2 (*continued*)

References	Application	Bacterial Strain	Cementation solution	Treating material	Testing
[143]	combating desertification	*Sporosarcina pasteurii (ATCC 11859)*	yeast extract (20 gL^{-1}), $(NH_4)_2SO_4$ (10 gL^{-1}), Tris buffer (0.13 $molL^{-1}$; pH 9.0), and urea (20 gL^{-1})	desert sand samples	XRD, SEM, sand fixation experiments, Compressive strength test
Internal and costal erosion control					
[49], [47]; [50]	internal erosion control in earth-filled embankment dams	*S. pasteurii (ATCC 6452)*	Urea- $CaCl_2$ (0·2 M, 0·4 M, 0·6 M, 1·0 M, 2·0 M), Nutrient broth 6 g/l	mixing a natural gravel soil with a British Standard graded sand	Internal erosion test
[102]	erosion mitigation and stabilisation of sandy soil foreshore slopes	*Sporosarcina pasteurii*	0.7 M $CaCl_2$ and urea served as fixation fluid and ce-mentation fluid	sandy soil was sourced from Troon beach in Ayrshire, UK	simulation of tidal cycles
[67]	increase erosion resistance of sand	*sporosarcina pasteurii (DSM 33)*	equimolar of calcium chloride and urea (1 mol/L)	the Qingdao Sea Sand, mainly composed of siliceous sand	bench-scale flume erosion tests, Penetration resistance test
[7]	erodibility improvement for beach sand	*S. pasteurii NRS929 (USDA)*	urea/ calcium (2.5 M)	beach sand collected from Atlantic Beach, Florida	erosion testing;acid-wash and control testing, crust-depth Testing
[75]	mitigating coastal sand dune erosion	*S. pasteurii, ATCC 11859*	0.5 M urea and 0.25 M $CaCl_2$	a commercial calcareous sand originated from the State of Hawaii	Small-scale laboratory model tests, erosion test
[104]	coastal protection	*Bacillus sp.*	-	Natural clean silica sand	Small-scale laboratory model tests
[124]	mitigate scouring/erosion of sand embankment in coastal areas	*Sporosarcina pasteurii*	Purified water 100 mL; Tryptone 1.5 g, Soy peptone 0.5 g, NaCl 0.5 g, Urea 2 g	sand from a construction site	Small-scale laboratory model tests, Scouring/erosion tests

biogrouting progress spatially and temporally without disturbing the ground. Cheng and Cord-Ruwisch [10] found that uniform cementation throughout the entire length of a 1-meter sand column required the percolation of alternating solutions containing bacteria or calcium ions. Martinez et al. [81] showed that injection of bacteria at a concentration of 7×10^5 cells/mL and an injection rate of 10 mL/min for 1.5 pore volumes followed by a 6-hour retention period was the most effective method for achieving uniform distribution in MICP experiments conducted in half-meter columns. Cheng and Cord-Ruwisch [11] conducted a 2-meter column MICP experiment and observed clogging close to the injection end when fine sand particles with diameters smaller than 0.3 mm were used, but not when the particle size was bigger than 0.5 mm. In a three-dimensional fine sand cementation trial, Cheng and Cord-Ruwisch [11] achieved a relatively homogeneous cementation to a depth of 20 cm in the horizontal direction, with 80% of the cemented sand having a strength between 2 and 2.5 MPa. Gomez et al. [35] demonstrated that biostimulation may yield comparable results to biocementation at the meter scale. Wu et al. [127] conducted biogrouting tests in 1 m3 models with pure silica sand and rock blocks filled with sand, achieving relatively uniform MICP treatment using low-pH single-phase injection [15] and high temperature single-phase injection methods [130] due to the bio-cementation process lag period. San Pablo et al. [103] suggested that lower ureolytic rates enhance the spatial uniformity and extent of biocementation.

Along with achieving homogeneity, recent advancements have addressed other challenges associated with Microbially Induced Calcium Carbonate Precipitation (MICP), including treating soils beyond sand, reducing by-product NH_4^+, and applying MICP in the field. For instance, Zamani and Montoya [138] found that the efficacy of MICP on silty sands relies on relative density, fines content, and soil fabric. Moon et al. [86] discovered that adding kaolin as a filler material increased contact points among particles, resulting in improved strength and stiffness of MICP-treated soils.

MICP has also been tested in simulated marine environments with high ion content [14,136], reduced oxygen availability [70], and temperature variance [93], as well as in calcareous sand [21,78] and marine clays [136]. Cheng et al. [14] demonstrated that seawater can be used instead of cementation solution for MICP. Yu and Rong [136] discovered that *Sporosarcina pasteurii* strains can multiply in seawater and have urease activity, making it possible to use MICP for constructing ocean islands and reefs far from the mainland. Li et al. [70] found that adequate air supply is essential to improve the MICP processes. Peng et al. [93] discovered that $CaCO_3$ precipitation at 10 ℃ was higher than that at 30 ℃, while Liu et al. [78] emphasized the importance of $CaCO_3$ content in increasing the strength and stiffness of MICP-treated calcareous sand. Cui et al. [21] found that precipitated calcium carbonate bonds particles, thereby enhancing the shear strength of calcareous sand. To remove the byproduct NH_4^+, Lee et al. [69] suggested using a high pH and high ionic strength rinse solution. Lastly, Terzis et al. [116] presented a full-scale application of slope stabilization via MICP followed by long-term GIS surveillance and concluded that MICP can be an efficient tool for improving the structure and performance of fine soils.

3.2. Liquefaction provision

Numerous researchers have analyzed the mechanisms of MICP in relation to soil liquefaction resistance. In 2013, Montoya et al. [85] discovered that sands treated with MICP demonstrated a significant increase in resistance to liquefaction. This was evidenced by a decrease in pore pressures and shaking-induced settlements, as well as an increase in maximum acceleration at the ground surface. The study also revealed a transition in soil behavior from soil-like to rock-like. Simatupang et al. [108] investigated the correlation between small-strain stiffness and liquefaction resistance, discovering two mechanisms that contributed to the enhanced resistance: (1) the calcite precipitated in

the sand bind the sand grains, thereby reducing strain and excess pore-pressure generated during the cyclic loading, and (2) the enhanced dilative nature of the sand due to the relative angularity provided by the calcite crystals or the ratio of the crystal size to grain size of the sand. Xiao et al. [129] also identified the factors contributing to improved resistance to liquefaction, which included an increase in surface roughness and filling of voids between particles.

Research has shown that carbonate content highly affects the liquefaction resistance of MICP-treated sand. For example, the number of cycles to liquefaction increased with increasing cementation content, and MICP treatment was shown to significantly reduce the liquefaction potential of calcareous sand [129]. In addition, Darby et al. [24] found that cone penetration resistances and shear wave velocities were sensitive to light, moderate, and heavy levels of cementation, and were able to capture the effects of cementation degradation. Sun et al. [112] found that as the $CaCO_3$ content increased, the number of cycles before liquefaction (NL) and residual strength (τ_r) increased exponentially, while the damping ratio (D) decreased exponentially. Moreover, the linear correlations between specific gravity and $CaCO_3$ content, N_L, τr and D can be established for MICP-solidified loess soil.

Apart from $CaCO_3$ content and properties, soil types, properties and saturation ratio also affect liquefaction resistance behavior of MICP-treated sand. Simatupang and Okamura [107] found that the lower the degree of saturation during calcite precipitation and the higher the calcite content in the samples, the higher the liquefaction resistance of the EICP-treated sand. He and Chu [43] found that reduction in the degree of saturation from 100% to a range of 95–88% more than doubled the undrained shear strength and lead to a transition from strain softening to strain hardening in the stress-strain behavior of sand with relative density Dr 10% and Dr 30%. Xiao et al. [129] found that the liquefaction resistance of clean calcareous sand may be significantly improved by MICP treatment. Zamani et al. [140] found that by applying MICP, the liquefaction resistance increases significantly for all amounts of fines tested, and that the treatment efficiency depends on the amount of fines present, which dictate the relative density and the fabric governing the structure. Similarly, Zamani and Montoya [139] found that the presence of fines by itself leads to generation of higher levels of pore-water pressure during the injection process, which necessitates higher strength improvement to prevent the development of excessive plastic strains. Therefore, improvement in shear strength and stiffness relative to the magnitude of the hydraulic conductivity level and their rate of change during the MICP process are key parameters in determining the radius of treatment. However, Karimian and Hassanlourad [55] found that the number of cycles required for inducing liquefaction after MICP treatment increases over five times for the sand sample and less for silty mixtures. Bio-treated samples are still liquefiable, but due to bonded clusters, their resistance has increased. In addition, Karimian and Hassanlourad [55] found that there is no significant difference in the amount of calcium carbonate precipitation between sand and silty sand, which means that the inclusion of fines in the sand does not notably affect the calcium carbonate content.

3.3. Dust and desertification control

Gomez et al. [36] conducted a field-scale study involving application of MICP to improve the erosion resistance of loose sand deposits and provide surface stabilization for dust control and future re-vegetation. Improvement was assessed to a depth of 40 cm using dynamic cone penetration (DCP) testing and measurements of calcite content. Hamdan and Kavazanjian [39] conducted wind tunnel tests to show that enzyme-induced carbonate precipitation (EICP) holds promise as a method for mitigation of fugitive dust emissions. Shi et al. [106] explored effects of MICP on prevention of mine dust and suggested that MICP has strong development prospects. Zomorodian [147] conducted bench-scale experiments and wind tunnel experiments investigating the effectiveness of MICP for stabilization of silica and carbonate sands and demonstrated that 28-day singly cured, MICP-spray-treated crustal sand layers were stable to simulated 20 $m \cdot s^{-1}$ winds measured at 20 cm above the surface layer. Li et al. [71] conducted laboratory and field MICP experiments and suggested that MICP can effectively rectify the shortcomings of straw checkerboard barrier (SCB) technology, and that combining both technologies for mitigating desertification should have promising outcomes by accelerating the process of sand fixation, vegetation restoration, and ecological restoration. Meng et al. [83] conducted MICP field tests on artificial mounds and bare sandy land located in Ulan Buh Desert, Ningxia Hui Autonomous Region, China and found that MICP could significantly enhance the bearing capacity and wind erosion resistance of surficial soil through the formation of soil crusts. Zhang et al. [143] showed that excess Mg^{2+} slightly promoted bacterial growth.

3.4. Internal and costal erosion control

In the study by Jiang and Soga [49], it was observed that MICP treatment effectively mitigated internal erosion in a soil containing 25% sand and 75% gravel. However, for specimens containing 50% sand and 50% gravel, MICP treatment was only successful with a specific injection method and at low axial stress. The efficiency of internal erosion reduction was found to be controlled by the calcium carbonate precipitation content in the soil, as suggested by Jiang and Soga [47]. Higher precipitation content resulted in larger clusters of cemented sand particles, thus reducing the likelihood of erosion. Jiang et al. [50] also found that MICP treatment reduced erosion and volumetric contraction in sand-clay mixtures and that the treatment was more effective in mixtures with a higher gap ratio due to their larger porosity.

Salifu et al. [102] demonstrated that MICP was effective in mitigating sediment detachment on steep slopes, which typically experience collapse due to tidal events. Kou et al. [67] found that cementation between sand particles increased the erosion resistance of sand. Chek et al. [7] found that higher optical densities, bacteria quantities relative to void volume, and bacteria quantities relative to urea led to lower erodibility and greater crust depth, while Liu et al. [74] found that MICP and enzymatic-induced carbonate precipitation (EICP) were effective in mitigating sand dune erosion, especially under mild-to-moderate wave and dune slope conditions. However, the effectiveness of MICP treatment deteriorated at steeper dune slopes exposed to prolonged periods of wave attack. Shahin et al. [104] performed lab-scale flume experiments that showed MICP was effective in preventing coastal erosion, and Wang et al. [124] found that MICP was efficient in protecting soil against rain erosion.

4. Construction remediation using MICP

MICP has a wide range of applications in the field of concrete and building material repairs. One area of research involves using MICP to deposit layers of $CaCO_3$ on surfaces to reduce water adsorption, fill cracks, or produce self-healing concrete. The relevant studies can be divided into two categories: (i) surface deposition and crack repair, and (ii) self-healing applications. Table 3 summarizes the research conducted in these areas, and Fig. 1(c) provides an illustration.

4.1. Surface deposition and repair of cracked samples

De Muynck et al. [25] conducted a study to evaluate the improvement in the durability of cementitious materials treated with MICP. They found that the surface deposition of calcium carbonate crystals reduced water absorption by 65–90%, depending on the porosity of the specimens. This, in turn, decreased the carbonation rate and chloride migration by about 25–30% and 10–40%, respectively. They also observed an increased resistance to freezing and thawing. In another study, De Muynck et al. [26] investigated the bio-treatment of concrete surfaces and demonstrated that the bacterial deposition of a calcite

Table 3
MICP as construction remediation materials.

Authors	Application	Bacterial Strain	Cementation solution	Treating material	Testing
Surface deposition and repairment of cracked samples					
[26]	Improvement of durability of cementitious materials	*B. sphaericus*	3 g/L nutrient broth (Oxoid N.V., Drongen, Belgium), 2.12 g/L $NaHCO_3$, 10 g/L ammonium chloride and 10 g/L urea	Mortar mixtures with a Portland cement (CEM I 52.5 N)	thin sections, SEM, water absorption, weight increase, permeability, accelerated carbonation test, freezing and thawing
[25]	Bacterial carbonate precipitation as an alternative surface treatment for concrete	*B. sphaericus*	0.3 L of supernatant was replaced by the same volume of tap water, containing 2 g/L nutrient broth powder, 10 g/L urea and 10 g/L SLM 1228	Mortar cubes/concrete cylinders	capillary water suction, permeability, colour measurement, contact angle, SEM, XRD
[3]	Surface treatment of concrete bricks	organic carbonate, dimethyl carbonate (DMC)	$CaCl_2$, DMC, NaOH	Concrete bricks	SEM, Water absorption tests, compressive strength, EDS
[6]	biomineralization for improving micro and macro-properties of concrete	*B. megaterium, B. pasteurii*	NB, NB and urea base	Concrete specimens	water absorption, volume of permeable voids and sulphate attack, flexural strength, splitting tensile strength, compressive strength
[18]	Mortar crack repair	*Sp. pasteurii*	urea-$CaCl_2$ solution was used at 0.2 M of concentration.	Mortar samples	splitting tensile test, calcium carbonate deposit, water permeability
[51]	crack healing performance in mortar	*Bacillus sphaericus*	78 mL of bacterial cells and 2.7 g of nutrient broth were dissolved in 0.375 M $CaCl_2$ to prepare the bacterial solution. The $NaHCO_3$ was added into the bacterial solution to control the pH at 8.	cubic mortar specimens	water permeability, microstructure study, crack observation, average velocity of ultrasonic wave propagation, compressive strength
[145]	improvement in properties of concrete with modified RCA	*Sp. cell*	20 g/L tryptone, 10 g/L NH_4Cl, 20 g/L urea, 2.12 g/L Na_2CO_3, and 0.55 mol/L $CaCl_2$	ordinary Portland cement, RCA	SEM, physical properties tests, steel corrosion in concrete, compressive strength, cracks observation, ITZs microhardness test
[68]	bio-bricks generations	*Sp. pasteurii* and human urease activity	urea-rich urine solution, additional calcium in the form of $CaCl_2$ and nutrient solution	dune sand sourced from Cape Town and Greywacke aggregate	Efficiency, urea hydrolysis rate, ammonium concentration monitoring, compressive strength
Self-healing concrete					
[98]	microbial self-healing concrete	spore-forming bacteria species		Portland cement	workability, repair rate, water permeability, field test methods
[119]	recycled concrete aggregates	*S. pasteurii*	modified mineral liquid medium (MM medium)	recycled concrete aggregates, ordinary Portland cement	water transport properties, Visualization and quantification of crack healing, Mechanical properties. XRD
[137]	zeolite as a bacterial carrier in the self-healing of cement mortar cracks	*B. cereus*	The liquid medium used in the experiment was 10 g/L peptone, 10 g/L NaCl, 20 g/L urea, and 10 g/ L glucose.	Natural zeolites, Ordinary Portland cement P.O 42.5	water resistance of ZMPs, effect of crack healing, water absorption, healing rate, permeability, detection of healing substances in cracks.
[109]	bio self-healing concrete	*Bacillus cereus*	Luria Bertani (LB) Medium and Urea Medium (UM)	mortar	compressive strength and crack generation, SEM, XRD

layer on the surface of the concrete specimens reduced capillary water uptake and permeability towards gas. The use of pure cultures was more effective in decreasing water uptake compared to the use of mixed ureolytic cultures as a paste. The results obtained with the species Bacillus sphaericus were similar to those obtained with conventional water repellents. Amidi and Wang [3] and Chaurasia et al. [6] also investigated the use of MICP for surface treatment of concrete, evaluating the efficiency of the resulting improvement in both microscale and macroscale properties of the materials. Amidi and Wang [3] used the organic carbonate dimethyl carbonate (DMC) as a means to provide the required carbonate for the generation of carbonate precipitants. Interestingly, instead of using a bacterial strain, DMC can be hydrolyzed into methanol and carbonate under basic pH conditions at ambient temperature and pressure.

Yang and Cheng [134] explored the use of microbial grouting as a reinforcement method for deteriorated masonry structures by injecting microorganisms and cementation solution into pores. They successfully produced mortars with maximum strength of 55 MPa that have superior mechanical properties and durability compared to conventional mortar. In addition, according to Choi et al. [18], MICP can be effectively utilized to repair cracks in mortar. The study demonstrated that the water permeability of cracked samples was reduced by the MICP repair technique, which is the primary objective in this application. The water tightness of the treated mortar was comparable to that of the mortar without any cracks [51]. Lambert and Randall [68] proposed using MICP in conjunction with human urease to generate bio-bricks. The resulting material was found to have a strength of up to 2.7 MPa, which is comparable to natural materials used for the same purposes. These innovative techniques have the potential to revolutionize the way cultural relics are repaired and preserved for future generations. According to Liu et al. [74], MICP improves tile water resistance by changing surface microstructure, and higher concentrations of bacteria and cementation provide better protection with a threshold, while offering durability with low impact on air permeability and color, making it an effective method to prevent the weathering of ancient tiles [77]. Meanwhile, Zhao et al. [145] investigated the application of MICP to enhance the durability and mechanical properties of recycled aggregate concrete (RAC). They employed the bacterial strain Sp. Cell to treat RCA with MICP, and the results showed that the treated RCA had reduced water absorption and apparent density, increased compressive strength, better steel corrosion resistance, and fewer corrosion-induced cracks. The authors attributed this improvement in performance to the enhanced microhardness of the interfacial transition zones (ITZ).

MICP and EICP are two techniques that have shown potential in repairing and protecting cultural relics such as compacted soil structures, rock buildings, and bricks. Zhang et al. [143] proposed the use of MICP or EICP for repairing these structures. MICP improves tile water resistance by changing surface microstructure. High bacteria and cementation concentrations improve protection, but with a threshold. MICP offers durability with low impact on air permeability and color, and can prevent weathering of ancient tiles. Liu et al. [74]. utilized an improved version of EICP technology with sucrose to prepare a surface protective material for tabia relics, a common building material in ancient China. This protective material was found to have superior performance compared to traditional EICP, with increased surface hardness, salt corrosion resistance, weather resistance, and water repellency.

4.2. Self-healing concrete

MICP has shown great potential in the development of self-healing concrete. Chetty et al. [17] reviewed the use of various MICP microorganisms as self-healing agents and highlighted the need for systematic and comparable evaluation methods. Intarasoontron et al. [45] used microencapsulated bacterial spores in specimens, but observed lower ultimate loads than control specimens. Qian et al. [98] utilized spray-dried fermented bacteria to produce powder-based and capsule-based microbial agents for concrete healing, which is more convenient than liquid-based agents. Wang et al. [119] used MICP to self-heal existing cracks in concrete by inserting free spores in a liquid solution, and noted that high urease-producing bacterial strains are required for this application. Yuan et al. [137] proposed the use of zeolite as a bacterial carrier in the self-healing of cement mortar cracks. Sohail et al. [109] studied the effectiveness of MICP for self-healing concrete at high temperatures and humidity. In all cases, necessary curing measures must be taken to keep the cracks wet and supply nutrients for the bacteria to achieve self-healing effects.

5. MICP for bioremediation purposes

The use of MICP for solidifying heavy metal ions such as Pb(II), Cu (II), Zn (II), Cd(II), Cv(VI), Ni(II), and As(III) through urea hydrolysis has proven to be successful. For instance, Chen et al. [9] explored the uptake and biomineralization of Pb(II) using *Bacillus cereus* 12–2 isolated from lead-zinc mine tailings. However, in some studies, alternative MICP mechanisms such as photosynthesis have been employed [144]. Zhao et al. [144] proposed that a bioreactor based on the precipitation of $CaCO_3$ induced by *N. calcicola* could be a promising and cost-effective approach for removing cadmium (Cd). This section provides an overview of the removal mechanism, efficiency, influencing factors, and bacterial toxicity of MICP for bioremediation purposes. Table 4 summarizes the relevant research, and Fig. 1(d) illustrates it.

There are several mechanisms involved in the removal of heavy metals using MICP, including: 1) pH increase to promote heavy metal precipitation; 2) bio-sorption; 3) co-precipitation of heavy metals with Ca^{2+} and 4) lead carbonate ($PbCO_3$) crystal formation. Firstly, the pH is increased by MICP, which promotes heavy metal precipitation. For example, Yang et al. [133] observed that MICP significantly increased the pH of treated mine tailing soil, leading to the precipitation and immobilization of toxic metals. Secondly, bio-sorption takes place during MICP, as demonstrated by Zhao et al. [144], who found that Cd^{2+} was primarily sequestered in the organic-bound fraction within the cells of *N. calcicola* bacteria. Jiang et al. [48] also suggested that the mechanism of Pb immobilization includes abiotic and biotic precipitation, as well as bio-sorption. Thirdly, co-precipitation of heavy metals with Ca^{2+} occurs during MICP. For example, Yang et al. [133] used X-ray diffraction (XRD) to confirm the presence of MICP products, such as calcite, gwihabaite, and aragonite, which could adsorb and co-precipitate with toxic metals. Zeng et al. [141] also used Fourier transform infrared spectroscopic and X-ray diffraction analyses to confirm that the precipitates were mostly calcite crystals, while lead was fixed as hydrocerussite. Additionally, Yin et al. [135] used XRD spectra to detect the precipitation of (Ca 0.67, Cd 0.33) CO_3 and calcite phases. Fourthly, precipitation of heavy metal carbonate was observed. Kang et al. [53] confirmed the presence of Pb along with carbon (C) and oxygen (O) within the $PbCO_3$ crystals using energy dispersive X-ray spectroscopy.

In general, MICP is highly efficient in removing heavy metals. For example, Mwandira et al. [89] achieved complete removal of 1036 mg/L of Pb^{2+} using MICP. Qian et al. [99] demonstrated 98.8% removal of 200 mg/L Pb using fungal-based MICP in just 12 days. He et al. [44] reported removal efficiencies of up to 86% for Pb(II) and 76.8% for Cr (VI) at an initial metal concentration of 25 mg l^{-1}. Peng et al. [92] used MICP to remove 99.50% of Cd within 7 days, while Zeng et al. [141] successfully remediated 25 mg/L Pb^{2+} and 5.6205 mg/L Cd^{2+} in a real landfill leachate using MICP.

Several factors have been found to impact the efficiency of removing heavy metals by MICP. For instance, Kang et al. [52] identified bacterial toxicity as a critical factor that may affect the removal efficiency of heavy metals using MICP. Mixtures of different bacterial strains showed higher growth rates, urease activity, and resistance to heavy metals than single culture methods. Jiang et al. [48] found that the calcium source and initial concentration of bacteria significantly influenced Pb

Table 4
MICP for bioremediation purposes.

Authors	Application	Bacterial Strain	Cementation solution	Treating material	Testing
Bioremediation in liquid media					
[5]	remediation of cadmium (II)	urease positive Serratia marcescens (NCIM2919) and Enterobacter cloacae EMB19 (MTCC10649)	Sterile nutrient media (50 mL) containing 25 mM (2774.5 mg L^{-1}) $CaCl_2$, 2% (v/v) (333.0 mM or 20,000 mg L^{-1}) urea, and 5.0 mg L^{-1} (0.0445 mM) of Cd (II)	Liquid containing Cadmium	Cadmium and calcium precipitation, mineralization estimation, EDX, SEM
[48]	immobilizing of Pb contaminants	Sporosarcina pasteurii	Stock solutions (1 M) were prepared using analytically pure reagents including $Pb(NO_3)_2$, $CaCl_2$, Ca (Ac)2 (i.e. calcium acetate) and urea.	Liquid medium containing Pb	Measurements of pH, electrical conductivity, urease activity, and viable cell number, Pb immobilization tests
[46]	Removal of Heavy Metals Zinc, Lead, and Cadmium by Biomineralisation	Sporosarcina pasteurii and Urease-Producing Bacteria Isolated from Iranian Mine Calcareous Soils	zinc (Zn), lead (Pb), and cadmium (Cd) from solutions with concentrations of 100, 300, and 500 mM of these metals' ions.	solutions containing contaminants	Heavy Metal Precipitation Experiments, SEM, EDS, MIC tests, Urease activity measurements
[29]	Ca-mediated alleviation of Cd^{2+} induced toxicity and improved Cd^{2+} biomineralization	Sporosarcina pasteurii	$CdCl_2$, $CaCl_2$, urea, $CuCl_2{\cdot}2\,H_2O$, $ZnCl_2{\cdot}7\,H_2O$, $MnCl_2{\cdot}4\,H_2O$ and $NiCl_2{\cdot}6\,H_2O$	liquid	Urease activity, SEM, EDS, Measurement of intracellular and extracellular cd concentration
[53]	Bioremediation of lead	Enterobacter cloacae	The 1 M Pb(II) stock solutions were prepared by dissolving the exact quantities of $PbCl_2$ in Milli-Q water and filtering through a 0.22 mm filter (Pall Co., MI, USA). Working concentrations of Pb(II) were obtained by serial dilution.	solutions containing Pb	Bacterial identification, biochemical tests, Impermeability test, calcite production measurements, urease activity, Pb precipitation
Bioremediation of contaminated soil					
[1]	Biomineralization based remediation of As(III)	Sporosarcina ginsengisoli	nutrient broth media containing 2% urea and 25 mM $CaCl_2$supplemented with 50 mM As_2O_3	soil was collected from nearby farmland	Arsenic sequential extraction procedure and analysis, XRD, ATR-FTIR spectroscopy
[8]	bioremediation of Pb polluted soil	*Bacillus pasteurii* ATCC 11859	bacterial agent group I (BS I: soil + medium + bacteria + 1 mol/L $CaCl_2$) and bacterial agent group II (BS II: soil + medium + bacteria + 1.5 mol/L $CaCl_2$)	high-concentration lead-contaminated soil around a gold mine tailing	pH, nitrogen content, CT scanning
[76]	Bioremediation of metal-contaminated soils	*Sporosarcina pasteurii* (*S. pasteurii*)	400 mL nutrient solution recommended by DSMZ (tryptone 15 g/L, soy peptone 5 g/L, and NaCl 5 g/L)	soils contaminated with lead (Pb), zinc (Zn) and cadmium (Cd).	Sequential extraction, Freeze-thawing, Surface water erosion, High temperature Acid rain tests
[133]	Bioimmobilization of Heavy Metals in Acidic Copper Mine Tailings Soil	Urease-producing bacteria were isolated from the acidic copper mine tailings samples	One g soil was inoculated into 50 mL nutrient broth (pH 8.0) containing 2% urea (w/v) and 25 mM $CaCl_2$ and incubated at 30 C for 96 h under shaking conditions	100 g toxic metal contaminated mine tailing soil	XRD, SEM, Bacterial growth, soil urease activity and pH were measured, the mine tailing samples were analyzed for Cu, Pb and Cd using an ICP-MS spectrometer
[135]	Inhibition of cadmium releasing from sulfide tailings	urease producing bacteria isolated from the soil-tailings	——	Samples collected from the copper mine	*Biomineralization tests, Microcosm experiments using SEM XRD, bacterial concentration measurements, Cd leaching tests*
[90]	Copper mine tailings valorization	*Sporosarcina pasteurii*	equimolar urea-calcium concentration	copper mine tailing samples received from a Greenfields copper mine project in Columbia	measurement of the depletion of calcium ions, cell density, compressive strength testings, SEM
[92]	immobilizing Cd in water and soil	Cd-resistant ureolytic bacterial strain isolated from the sediment of an acid wastewater ditch in a pyrite mining area.		soil and water	Cd removal, preicipitates characterisation, Soil microecology analysis
[100]	Multiple heavy metals immobilization	bacterial isolates	The bacterial suspension (1 mL) was added to 1 mL of calcium chloride dihydrate solution (0.350 M) containing 2 mL of urea solution (3 M).	soil sample used for ureolytic bacteria isolated collected pyrite mine sites	sequencing of bacteria, heavy metal toxicity testing, urease activity, precipitation analysis XRD
[141]	mineralization of lead and cadmium in landfill leachate	*Sporosarcina pasteurii*	20 g/L urea, 50 mM Ca^{2+}, 20 mg/L Pb^{2+}, and a 2% (*v*/*v*) bacterial resuspension solution	synthetic landfill leachate (SLL) contaminated by Pb^{2+}, 100% of the 20 mg/L Pb^{2+}	SEM, EDS, Fourier transform infrared spectroscopic and X- ray diffraction analyses, urease activity

immobilization efficiency, while Peng et al. [92] observed that initial pH and Cd concentration were important parameters that influenced Cd removal rate. Fang et al. [29] found that Ca^{2+} supplementation notably improved Cd^{2+} removal efficiency by about 100%. Moreover, the effects of the same parameters on different heavy metals are variable. For example, Mugwar et al. [87] reported that pH elevation and calcium precipitation strongly affected the removal of zinc and cadmium, but only partially affected the removal of lead and copper. Qiao et al. [100] found that Cd removal was mainly due to the formation of cadmium carbonate, Cu removal was dependent on the pH increase, while the precipitation that contributed to Zn and Ni removal was more complex. Qiao et al. [100] also found that the toxicity of these heavy metals to MICP bacteria was, from most to least toxic, Cd > Zn > Ni > Cu. Furthermore, Chen et al. [8] found that interactions between bioremediation and soil properties affected the efficiency of removing heavy metals from soils. Oliveira et al. [90] found that particle size was a key deciding factor and that MICP was not suitable for small particles (< 100 μm), such as mine tailings.

Compared to other methods for heavy metal remediation, MICP offers several advantages. According to Gadd [32], MICP can overcome some of the limitations associated with biosorption. When heavy metals are precipitated with biogenic minerals, they are usually incorporated into the lattice of mineral crystals, making them geologically stable. This was demonstrated in a study by Zhao et al. [144], where Pb-MICP precipitates were stable under continuous acid degradation (pH = 5.5), and only 1.76% of the lead was released after 15 days. Additionally, MICP offers a low-cost and eco-friendly method for heavy metal remediation through bio-immobilization of lead [89]. In terms of solidifying heavy metal contaminated soils, Han et al. [40] found that MICP contributes to better strength improvement, while retaining better water permeability and higher durability, and rarely damages the original soil structure during grouting, making it more environmentally friendly compared to other agglutinate binders.

Despite its advantages, there are also challenges facing MICP. Firstly, it is important to optimize the dosage of urea and the recovery of ammonium to improve the economic and environmental benefits of the MICP process [141]. Secondly, there is a need to assess the longer-term performance of heavy metal removal by MICP [144]. Finally, the high costs of reactant materials, the uneven effect in large-scale fields, destruction of the ecological equilibrium, and uncertain adaptability to complex environments also need to be considered [40].

6. Material modification and protection

Table 5 summarizes research on the use of MICP for material modification and protection, while Fig. 1(e) provides an illustration of the findings. MICP can alter the physical properties of soil surfaces, making it a valuable tool for modifying and protecting materials.

6.1. Preventing the corrosion of marine materials

Recently, MICP has shown promise in protecting steel from corrosion in marine engineering applications. By forming a dense mineralized layer on the steel surface, MICP can prevent corrosive agents in the environment from directly contacting the steel surface, inhibiting metal corrosion. *Pseudoalteromonas lipolytica*, a bacterium that can form an organic-inorganic hybrid film composed of calcite and EPS, has been observed to aid in forming a dense mineralized layer on the steel surface, inhibiting corrosion and exhibiting self-healing properties [78]. Guo et al. [38] found that adding 0.6 wt% molybdenum in steel could enhance the mineralization process, as molybdenum ions acted as chemoattractants of *Pseudoalteromonas lipolytica* and activated the chemotaxis pathway. The resulting uniform and dense biomineralized layer effectively inhibited pitting corrosion. In a multi-bacterial environment, *Pseudoalteromonas lipolytica* mixed with *Bacillus subtilis* or *Pseudomonas aeruginosa* showed excellent corrosion protection for steel, forming a more compact and denser carbonate layer than single bacteria and exhibiting better anti-corrosion properties for steel [37]. *Bacillus cereus* was found to form an EPS film on the surface of stainless steel that interacted with metal ions in solution to inhibit metal corrosion [72]. Methanogenic bacteria extracted from buried steel piles resulted in the formation of a dense, corrosion-resistant carbonate layer on the surface of the piles [56]. Salinity is a factor that must be considered in the marine environment, as *Bacillus subtilis* and *Bacillus safensis* displayed the maximal anti-corrosion effect on steel bars in a 3.5% sodium chloride solution [54].

6.2. Oil and water separation

The preparation of super-wetting materials is crucial for effectively treating marine oil spills, and the roughness of the material surface plays a significant role. An increase in surface roughness leads to an increase in wettability. MICP produces calcium carbonate, which has inherent hydrophilicity and high surface roughness, making it an excellent material for creating super-wetting oil-water separation materials. Tang et al. [113] utilized MICP to fabricate a superhydrophobic calcium carbonate-coated stainless steel mesh (SSM) and then modified the surface with stearic acid (SA) for oil-water separation. The surface roughness was confirmed by SEM and white light interferometry. The superhydrophobic mesh exhibited high oil fluxes ($0.2–9.12 \times 10^4$ $L{\cdot}m^{-2}{\cdot}h^{-1}$), high separation efficiencies (> 94.8%), excellent wear resistance, outstanding anti-pollution performance, and promising anti-icing properties. In a subsequent study, Tang et al. [114] successfully produced a dense and continuous layer of mineralized calcium carbonate on the surface of a stainless-steel mesh using *Shewanella algae*. They observed that the steel mesh could achieve oil-water separation on the eighth day of mineralization, and the prepared mesh had a very high permeation flux ($1.55 \times 105\ L{\cdot}m^{-2}{\cdot}h^{-1}$) and high separation efficiency (≥98.5%).

6.3. Energy piles and ground source heat pumps

Researchers have investigated the use of MICP as a method of enhancing soil-pile heat exchange rates by improving the thermal properties of soil. Venuleo et al. [118] observed that the thermal conductivity of MICP-treated soil was significantly improved, particularly for low degrees of saturation. The improvement is attributed to the mineralized calcite crystals acting as 'thermal bridges' between soil grains, offering a larger surface area for heat exchange than untreated material where exchanges occur through smaller contact points. Martinez et al. [80] showed that the thermal conductivity of surrounding soils is crucial for the efficiency of energy piles and ground source heat pumps, and using MICP resulted in a significant increase in thermal conductivity (up to 330%) as calcite content increased. Wang et al. [125] also found that the thermal conductivity of sands increased significantly after MICP treatment, and the improvement was more significant with an increase in the number of treatment cycles. This enhancement is attributed to the MICP-induced $CaCO_3$ crystals functioning as 'thermal bridges' among sand grains, which provides a more effective heat transfer path and increases surface contact area in heat exchange processes. Cheng et al. [16] further suggested that using MICP as a soil improvement technique can effectively improve the thermal conductivity of soil surrounding energy piles, which has high potential to enhance the efficiency of energy piles.

6.4. Artificially made rock

The MICP method has been suggested as a potential manufacturing technique for creating customizable porous media, since coring can be costly and may destroy cementation [66]. The method has been successful in creating specimens with varying hydraulic conductivity, porosity, and strength by using different base materials with varying

Table 5
Material modification and protection.

Authors	Application	Bacterial Strain	Cementation solution	Treating material	Testing
Prevention of corrosion of metals in marine environments					
[4]	bio-based surface healing of structural repair cement mortars in maritime environments	*S. Pasteurii*	nutrient broth 4 g, NH_4Cl 10 g, $NaHCO_3$ 2.15 g, urea 20 g, distilled water 100 mL	Portland cement mortar CEM I 42.5 beams	Moisture buffering test, porosity, capillary test, UCS, SEM
[31]	mortar-crack repair in maritime environments	*S. Pasteurii*	Grade II 42.5 R Portland cement (OPC), urea, DE, BP, YE, calcium lactate and basalt fibre		three-point bending tests, water-flow tests, microscopic investigation
[54]	corrosion inhibition of steel bars by biofilm forming bacteria in corrosive environment	*B. subtilis, B. pumilus, B. australimaris and B. safensis*	consisted of 50 g/L calcium lactate, 4 g/L yeast extract, with 0%, 1.5%, 3.5% and 5% concentrations of so- dium chloride	Electrochemical performance of rebars	Surface analysis of rebars, Quantification of EPS, EDS, SEM
[38]	biofilm-induced mineralization on low alloy steel surface	*Pseudoalteromonas lipolytica*	2216E medium containing 35.000 g of NaCl, 0.500 g of KH_2PO_4, 0.060 g of $CaCl_2{\cdot}6\,H_2O$, 2.000 g of $MgSO_4{\cdot}7\,H_2O$, 1.000 g of yeast extract, 0.004 g of $FeSO_4{\cdot}7\,H_2O$, and 0.300 g of sodium citrate in 1 L of deionized water at 37 °C	steels	profilometry, EDS, Electrochemical measurements,Motility, chemotaxy assays and biofilm assay
[37]	synergistic biomineralization to inhibit steel corrosion in marine environments	*Two marine bacterial strains mixed with P. lipolytica: Bacillus subtilis and Pseudomonas aeruginosa*	2216E medium required for the bacteria, which had the following composition in g/L: 1.0 yeast extract, 5.0 peptone, 0.1 ferric citrate, 19.40 NaCl, 5.90 $MgCl_2$, 3.24 Na_2SO_4, 1.80 $CaCl_2$, 0.55 KCl, 0.16 Na_2CO_3, 0.08 $SrBr_2$, 0.08 KBr, 0.034 $SrCl_2$, 0.022 H_3BO_3, 0.004 $NaSiO_3$, 0.0024 NaF, 0.0016 NH_4NO_3, and 0.008 $Na_2\,HPO_4$.	low-alloy steel for marine engineering	surface characterisation, Electrochemical and weight loss measurements
[78]	The addition of copper accelerates the corrosion of steel via impeding T biomineralized film formation of Bacillus subtilis in seawater	*Bacillus subtilis*	marine broth (2216E medium)	low-alloyed steel plates	XRD, optical profilometry, electrochemical methods such as OCP, potentiodynamic po-larization and EIS, Measurement of metabolic production amount
[113]	Fabrication of calcium carbonate coated-stainless steel mesh for efficient oil- T water separation	*B. subtilis*	peptone (5.0 $g{\cdot}L^{-1}$), yeast extract (1.0 $g{\cdot}L^{-1}$), ferric citrate (0.1 $g{\cdot}L^{-1}$), sodium chloride (19.45 $g{\cdot}L^{-1}$), magnesium chloride (5.98 $g{\cdot}L^{-1}$), sodium sulfate (3.24 $g{\cdot}L^{-1}$), calcium chloride (1.8 g·L − 1), potassium chloride (0.55 $g{\cdot}L^{-1}$), sodium carbonate (0.16 $g{\cdot}L^{-1}$), potassium bromide (0.08 $g{\cdot}L^{-1}$), cesium chloride (0.034 $g{\cdot}L^{-1}$), boric acid (0.022 $g{\cdot}L^{-1}$), sodium silicate (0.004 $g{\cdot}L^{-1}$), sodium fluoride (0.0024 $g{\cdot}L^{-1}$), ammonium nitrate (0.0016 $g{\cdot}L^{-1}$), and disodium hydrogen phosphate (0.008 $g{\cdot}L^{-1}$).	superhydrophobic calcium carbonate ($CaCO_3$) coated-stainless steel mesh (SSM)	SEM, XRD, Fourier transform infrared spectroscopy (FTIR), Oil-water separation tests, Wear resistance tests, Anti-pollution tests, Anti-Icing tests
[28]	microbial enhanced oil recovery (MEOR)	*Bacillus megaterium, Bacillus licheniformis*	Glucose Mineral Salt Medium (GMSM)		Assessment of EOR application potential of biosurfactant
Energy piles					
[118]	energy piles and ground source heat pumps	*Sporosarcina pasteurii*	0.25 M urea, 0.25 M $CaCl_2$, 3 g/L NB, 10 g/L Ammonium chloride	silica sand/ different degrees of saturation	Thermal conductivity and shear wave velocity measurements, hanging column tests with SWRC measurements
[80]	energy piles and ground source heat pumps	*Sporosarcina pasteurii*	0·2 g/l yeast extract, 100 mM ammonium chloride, 350 mM urea and 250 mM calcium chloride was applied to each soil column.	sand	Thermal Conductivity Analysis, SEM

(*continued on next page*)

Table 5 (*continued*)

Authors	Application	Bacterial Strain	Cementation solution	Treating material	Testing
[16]	Bio-Cementation for Improving Soil Thermal Conductivity	*Bacillus sp.*	1 M urea, various combinations of $CaCl_2$ and $MgCl_2$	silica sand & fibre	thermal conductivity of soils
[125]	Thermal conductivity of sands	*Sporosarcina pasteurii*	1 M urea, 1 M $CaCl_2$	sand	Dual probe heat pulse (DPHP) sensor, thermal conductivity
[16]	Improving Soil Thermal Conductivity	*Bacillus sp.*	1 M urea, different combinations of $CaCl_2$ and $MgCl_2$ (0–1 M)	Silica sand	Thermal Conductivity, SEM
Artificially made sandstone for civil, energy, hydraulic and hydrological applications					
[91]	Mechanical properties of biologically cemented sandstone	*Sporosarcina pasteurii*	solutions containing reagents urea and calcium chloride	Silica sand	UCS, triaxial testing, tensile strength
[59]	Hydraulic fracturing experiments on bio-treated porous media	*Sporosarcina pasteurii*	0.375 M of urea, 0.25 M of calcium chloride ($CaCl_2$), and 3 g/L of nutrient broth	fine, medium-grained, coarse, very coarse sand, fine, coarse glass beads, angular sand	UCS, Point load tests, porosity, SEM, tensile strength, fracture toughness, fluid flow experiments
[64]	Hydraulic and mechanical properties of bio-treated porous media	*Sporosarcina pasteurii*	0.375 M of urea, 0.25 M of calcium chloride ($CaCl_2$), and 3 g/L of nutrient broth	Very fine, fine, medium-grained, coarse, very coarse sand, fine, coarse glass beads, angular sand	hydraulic conductivity, porosity, UCS, microCT scanning
[65]	Bio-cemented artificial sandstone generation	*Sporosarcina pasteurii*	0.375 M of urea, 0.25 M of calcium chloride ($CaCl_2$), and 3 g/L of nutrient broth	fine and very coarse sand	UCS, Point load tests, porosity, SEM
[62]	Bio- cemented artificial sandstone generation (tensile strength)	*Sporosarcina pasteurii*	0.375 M of urea, 0.25 M of calcium chloride ($CaCl_2$), and 3 g/L of nutrient broth	fine and very coarse sand	Tensile strength, surface roughness
[66]	Bio-cemented artificial sand generation	*Sporosarcina pasteurii*	0.375 M of urea, 0.25 M of calcium chloride ($CaCl_2$), and 3 g/L of nutrient broth	very coarse sand	Uniformity, flow rate, pH, quantitative polymerase chain reaction (qPCR), Ammonia Concentration
[33]	bio-cemented artificial sandstone generation - numerical modelling of UCS behaviour	*Sporosarcina pasteurii*	0.375 M of urea, 0.25 M of calcium chloride ($CaCl_2$), and 3 g/L of nutrient broth	very coarse sand	DEM-LLIGGGHTS modelling of UCS and Hydraulic fracturing
[63]	Fluid injection experiments for reservoir engineering applications	*Sporosarcina pasteurii*	0.375 M of urea, 0.25 M of calcium chloride ($CaCl_2$), and 3 g/L of nutrient broth	fine sands (Fraction D British Standards)	Infiltration/Fracture testing under true triaxial testing
[60]	fluid flow experiments in porous biocemented artificial sands for hydrology applications	*Sporosarcina pasteurii*	0.375 M of urea, 0.25 M of calcium chloride ($CaCl_2$), and 3 g/L of nutrient broth	fine, medium-grained, coarse, very coarse sand, fine glass beads	fracture propagation observation, pressure profile response

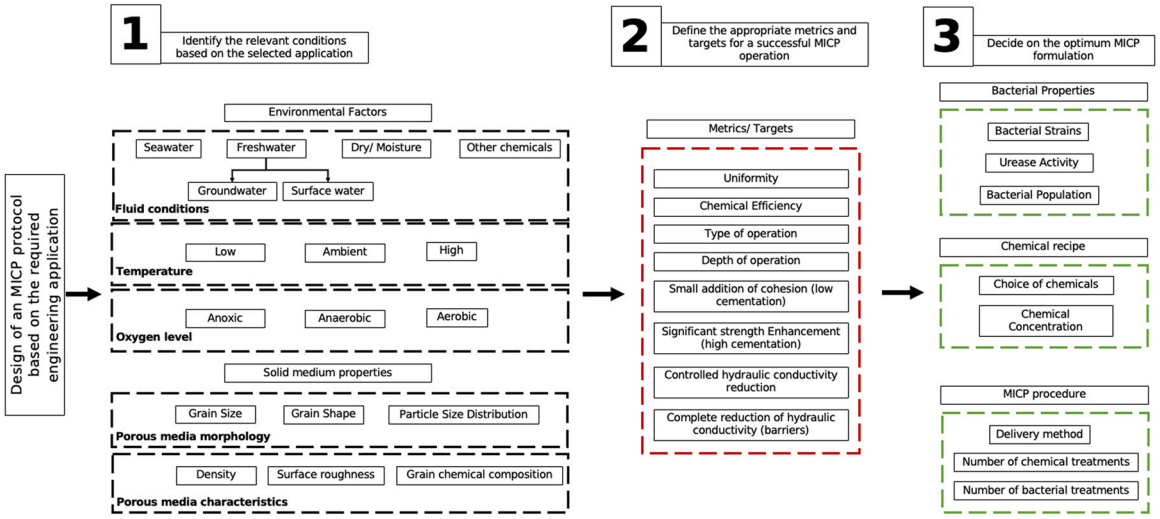

Fig. 2. Choosing an appropriate MICP design scheme based on the required application.

grain shapes, sizes, and particle size distributions [64]. Tests have been conducted to measure parameters such as tensile strength, unconfined compressive strength, stiffness, and the failure envelope [91,61,65,62,64].

Additionally, bio-treated specimens have been used successfully in fluid flow experiments for applications in energy, hydraulics, and hydrology [60,63]. In the case of unconventional reservoirs, safety is a primary concern when conducting fluid injection programs. These reservoirs are often comprised of weakly cemented sands found in intermediate depths in the groundwater zone. Precise distribution of various compounds (foams, emulsified oils, aqueous colloidal silica suspensions, etc.) at the target site is crucial to the effectiveness of in situ groundwater treatment. Injection programs aimed at remediating contaminated groundwater must take into account factors like hydraulic conductivity, porosity, and strength in order to prevent grain displacement or fracture. Konstantinou [59], Konstantinou and Biscontin [61], and Konstantinou et al. [63] have utilized MICP to produce realistic artificial weak sandstones or weakly cemented sands for laboratory testing of fluid injection relevant to the aforementioned applications. The infiltration/fracturing behavior of these materials differed substantially from competent materials, with significant leak-off and main cavity openings with multiple offshots. MICP-treated specimens allowed this behavior to be observed for the first time, whereas previously only cohesionless sand or hard sandstone were typically used in testing. The authors found that cemented specimens with greater hydraulic conductivity and larger pore networks were more difficult to crack due to excessive infiltration dominance, which prevented the development of the necessary pressure for fracture [60].

7. Choosing an appropriate MICP design scheme based on the required application, and potential new MICP applications

To design an effective MICP protocol, several factors must be considered, such as bacterial properties, chemical recipe, delivery of solutions, and MICP treatment parameters. These factors should be chosen based on the desired application and the success criteria, including chemical efficiency, strength enhancement, hydraulic conductivity reduction, impermeable barrier generation, and targeted depth of operation. However, before defining the procedure, other factors should be evaluated, such as environmental conditions and the properties of the solid medium.

To develop an MICP protocol, three aspects should be taken into account: identifying the relevant environmental conditions and properties of the porous medium, defining the target, and determining the optimal MICP formulation. Selecting appropriate bacterial strains is crucial for the procedure to survive various fluid conditions, such as seawater, freshwater, dry or undersaturated porous media, or the presence of other chemical components. For instance, in deep ocean sea beds, Hata et al. [41] isolated Sporosarcina newyorkensis, a ureolysis bacteria. A proposed methodology for designing an MICP procedure is shown in Fig. 2, and this section provides examples of how the MICP process is influenced by both the target application and environmental conditions.

The choice of bacterial strain for MICP is influenced by several factors, including oxygen levels, the presence of other chemicals, and the targeted application. For instance, the selection of bacteria will differ depending on whether the conditions are aerobic, anaerobic, or anoxic. Different bacteria, such as *S. pasteurii*, *E. aerogenes*, *P. fluorescens*, *Pseudomonas denitrificans*, *Alcaligenes*, *Denitro bacillus*, and *Thiobacillus*, may be used for different conditions.

Bacterial toxicity and its impact on heavy metal removal can complicate the definition of an optimal MICP formulation. Controlling permeability requires adjusting $CaCO_3$ production and its characteristics, which is influenced by bio-chemical factors, injection technique, and porous medium properties. To achieve a lower decrease in hydraulic conductivity, slower reactions, lower urease activities, and lower chemical solution concentrations are recommended. On the other hand, high urease activity, high flow rates, and sufficient chemical solution concentrations are necessary to generate an impermeable barrier.

For self-healing concrete and crack repairment applications, high bacterial populations and urease activity are essential. In contrast, uniform behaviour is required for intermediate depths in the ground. A balance of high flow rates and lower reaction rates involving bacteria with lower urease activities has been shown to be effective in achieving this. Porous medium configuration and properties also affect the MICP treatment process, and medium-grained particles are considered ideal for bio-cementation.

In addition to existing applications, future applications such as reparation of roads and pavements, protecting water distribution pipes from movement and corrosion, generating a barrier to prevent seawater intrusion, and protecting monuments from acidic rainfall could be designed based on the considerations discussed above.

8. Conclusions

While urea hydrolysis has been the primary method for studying MICP, other potential methods and combinations of methods need to be explored for more cost-effective and efficient MICP mechanisms to become commercially viable. Although individual factors affecting soil stabilization using MICP have been extensively researched, the impact of combined factors and varying environmental conditions still needs

further exploration.

The influence of local bacterial strains on MICP efficacy also requires more investigation, along with optimizing processing procedures for homogeneity and efficiency in large-scale applications. Demonstrating MICP's effectiveness in real-world applications is crucial before it can be widely adopted.

While MICP has been applied in various fields such as geotechnical engineering, environmental remediation, and oil and gas extraction, there are still many areas that have yet to be explored. For example, MICP could be combined with fluid injection techniques to address sea water intrusion or groundwater recharge, for underground hydrogen storage, or to immobilize contaminants or NAPLs in contaminated aquifers. MICP could also be used in combination with other construction methods such as artificial ground freezing, or for sand prediction and control during natural gas production. Further MICP could be used for ocean negative carbon emission [142].

Despite its challenges, including its environmental impact and operating system standards, MICP has shown progress and potential to be an environmentally friendly biotechnology in the near future. A proposed methodology for designing appropriate MICP treatment protocols can aid in its widespread adoption.

Declaration of Competing Interest

The authors declare that they have no known competing financial interests or personal relationships that could have appeared to influence the work reported in this paper.

Acknowledgments

Y. W. acknowledges the financial support of Natural Science Foundation of China (Grant No. 52171262) and Science and Technology Innovation Committee of Shenzhen (Grant No. JCYJ20210324103812033) for conducting this study.

References

[1] V. Achal, X. Pan, Q. Fu, D. Zhang, Biomineralization based remediation of As(III) contaminated soil by Sporosarcina ginsengisoli, J. Hazard. Mater. 201–202 (2012) 178–184, https://doi.org/10.1016/j.jhazmat.2011.11.067

[2] A. Al Qabany, K. Soga, C. Santamarina, Factors affecting efficiency of microbially induced calcite precipitation, J. Geotech. Geoenviron. Eng 138 (8) (2012) 992–1001, https://doi.org/10.1061/(asce)gt.1943-5606.0000666

[3] S. Amidi, J. Wang, Surface treatment of concrete bricks using calcium carbonate precipitation, Constr. Build. Mater. 80 (2015) 273–278, https://doi.org/10.1016/j.conbuildmat.2015.02.001

[4] J.M. Bergh, B. v.d., Miljević, O. Šovljanski, S. Vučetić, S. Markov, J. Ranogajec, A. Bras, Preliminary approach to bio-based surface healing of structural repair cement mortars, Constr. Build. Mater. (2020) 248, https://doi.org/10.1016/j.conbuildmat.2020.118557

[5] A. Bhattacharya, S.N. Naik, S.K. Khare, Harnessing the bio-mineralization ability of urease producing Serratia marcescens and Enterobacter cloacae EMB19 for remediation of heavy metal cadmium (II), J. Environ. Manage. 215 (2018) 143–152, https://doi.org/10.1016/j.jenvman.2018.03.055

[6] L. Chaurasia, V. Bisht, L.P. Singh, S. Gupta, A novel approach of biomineralization for improving micro and macro-properties of concrete, Constr. Build. Mater. 195 (2019) 340–351, https://doi.org/10.1016/j.conbuildmat.2018.11.031

[7] A. Chek, R. Crowley, T.N. Ellis, M. Durnin, B. Wingender, Evaluation of factors affecting erodibility improvement for MICP-treated beach sand, J. Geotech. Geoenviron. Eng 147 (3) (2021), https://doi.org/10.1061/(asce)gt.1943-5606.0002481

[8] M. Chen, Y. Li, X. Jiang, D. Zhao, X. Liu, J. Zhou, Z. He, C. Zheng, X. Pan, Study on soil physical structure after the bioremediation of Pb pollution using microbial-induced carbonate precipitation methodology, J. Hazard. Mater. 411 (2021) 125103, https://doi.org/10.1016/j.jhazmat.2021.125103

[9] Z. Chen, X. Pan, H. Chen, X. Guan, Z. Lin, Biomineralization of Pb(II) into Pb-hydroxyapatite induced by Bacillus cereus 12-2 isolated from Lead-Zinc mine tailings, J. Hazard. Mater. 301 (2016) 531–537, https://doi.org/10.1016/j.jhazmat.2015.09.023

[10] L. Cheng, R. Cord-Ruwisch, In situ soil cementation with ureolytic bacteria by surface percolation, Ecol. Eng. 42 (2012) 64–72, https://doi.org/10.1016/j.ecoleng.2012.01.013

[11] L. Cheng, R. Cord-Ruwisch, Upscaling effects of soil improvement by microbially induced calcite precipitation by surface percolation, Geomicrobiol. J. 31 (5) (2014) 396–406, https://doi.org/10.1080/01490451.2013.836579

[12] L. Cheng, M.A. Shahin, Urease active bioslurry: a novel soil improvement approach based on microbially induced carbonate precipitation, Canadian Geotechnical Journal 53 (9) (2016) 1376–1385, https://doi.org/10.1139/cgj-2015-0635

[13] L. Cheng, R. Cord-Ruwisch, M.A. Shahin, Cementation of sand soil by microbially induced calcite precipitation at various degrees of saturation, Canadian Geotechnical Journal 50 (1) (2013) 81–90, https://doi.org/10.1139/cgj-2012-0023

[14] L. Cheng, M.A. Shahin, R. Cord-Ruwisch, Bio-cementation of sandy soil using microbially induced carbonate precipitation for marine environments, Géotechnique 64 (12) (2014) 1010–1013, https://doi.org/10.1680/geot.14.T.025

[15] L. Cheng, M.A. Shahin, J. Chu, Soil bio-cementation using a new one-phase low-pH injection method, Acta Geotech 14 (3) (2018) 615–626, https://doi.org/10.1007/s11440-018-0738-2

[16] L. Cheng, N. Afur, M.A. Shahin, Bio-cementation for improving soil thermal conductivity, Sustainability 13 (18) (2021), https://doi.org/10.3390/su131810238

[17] K. Chetty, S. Xie, Y. Song, T. McCarthy, U. Garbe, X. Li, G. Jiang, Self-healing bioconcrete based on non-axenic granules: A potential solution for concrete wastewater infrastructure, J. Water Process Eng (2021) 42, https://doi.org/10.1016/j.jwpe.2021.102139

[18] S.-G. Choi, K. Wang, Z. Wen, J. Chu, Mortar crack repair using microbial induced calcite precipitation method, Cem. Concr. Compos. 83 (2017) 209–221, https://doi.org/10.1016/j.cemconcomp.2017.07.013

[19] J. Chu, V. Ivanov, V. Stabnikov, B. Li, Microbial method for construction of an aquaculture pond in sand, Géotechnique 63 (10) (2013) 871–875, https://doi.org/10.1680/geot.SIP13.P.007

[20] M.-J. Cui, J.-J. Zheng, R.-J. Zhang, H.-J. Lai, J. Zhang, Influence of cementation level on the strength behaviour of bio-cemented sand, Acta Geotech 12 (5) (2017) 971–986, https://doi.org/10.1007/s11440-017-0574-9

[21] M.-J. Cui, J.-J. Zheng, J. Chu, C.-C. Wu, H.-J. Lai, Bio-mediated calcium carbonate precipitation and its effect on the shear behaviour of calcareous sand, Acta Geotech 16 (5) (2020) 1377–1389, https://doi.org/10.1007/s11440-020-01099-0

[22] A.B. Cunningham, A.J. Phillips, E. Troyer, E. Lauchnor, R. Hiebert, R. Gerlach, L. Spangler, Wellbore leakage mitigation using engineered biomineralization, Energy Procedia 63 (2014) 4612–4619, https://doi.org/10.1016/j.egypro.2014.11.494

[23] M.O. Cuthbert, L.A. McMillan, S. Handley-Sidhu, M.S. Riley, D.J. Tobler, V.R. Phoenix, A field and modeling study of fractured rock permeability reduction using microbially induced calcite precipitation, Environ. Sci. Technol. 47 (23) (2013) 13637–13643, https://doi.org/10.1021/es402601g

[24] K.M. Darby, G.L. Hernandez, J.T. DeJong, R.W. Boulanger, M.G. Gomez, D.W. Wilson, Centrifuge model testing of liquefaction mitigation via microbially induced calcite precipitation, J. Geotech. Geoenviron. Eng 145 (10) (2019), https://doi.org/10.1061/(asce)gt.1943-5606.0002122

[25] W. De Muynck, K. Cox, N.D. Belie, W. Verstraete, Bacterial carbonate precipitation as an alternative surface treatment for concrete, Constr. Build. Mater. 22 (5) (2008) 875–885, https://doi.org/10.1016/j.conbuildmat.2006.12.011

[26] W. De Muynck, D. Debrouwer, N. De Belie, W. Verstraete, Bacterial carbonate precipitation improves the durability of cementitious materials, Cem. Concr. Res. 38 (7) (2008) 1005–1014, https://doi.org/10.1016/j.cemconres.2008.03.005

[27] T.D. DeJong, B.F. Michael, N. Klaus, Microbially Induced Cementation to Control Sand Response to Undrained Shear, J. Geotech. Geoenviron. Eng. 132 (11) (2006), http://dx.doi.org/10.1061/(ASCE)1090-0241(2006)132:11(1381).

[28] G. Dhanarajan, V. Rangarajan, C. Bandi, A. Dixit, S. Das, K. Ale, R. Sen, Biosurfactant-biopolymer driven microbial enhanced oil recovery (MEOR) and its optimization by an ANN-GA hybrid technique, J. Biotechnol. 256 (2017) 46–56, https://doi.org/10.1016/j.jbiotec.2017.05.007

[29] L. Fang, Q. Niu, L. Cheng, J. Jiang, Y.-Y. Yu, J. Chu, V. Achal, T. You, Ca-mediated alleviation of Cd^{2+} induced toxicity and improved Cd2+ biomineralization by Sporosarcina pasteurii, Sci. Total Environ. (2021) 787, https://doi.org/10.1016/j.scitotenv.2021.147627

[30] Ferris, F.G., Stehmeier, L.G. Bacteriogenic Mineral Plugging: U.S. Patent 5143155[P]. 1992-9–1.

[31] Q. Fu, Y. Wu, S. Liu, L. Lu, J. Wang, The adaptability of Sporosarcina pasteurii in marine environments and the feasibility of its application in mortar crack repair, Constr. Build. Mater. (2022) 332, https://doi.org/10.1016/j.conbuildmat.2022.127371

[32] G.M. Gadd, Bioremedial potential of microbial mechanisms of metal mobilization and immobilization, Curr. Opin. Biotech. 11 (2000) 271–279, https://doi.org/10.1016/S09581669(00)00095-1

[33] P.A. Gago, C. Konstantinou, G. Biscontin, P. King, A numerical characterisation of unconfined strength of weakly consolidated granular packs and its effect on fluid-driven fracture behaviour, Rock Mech. Rock Eng 55 (8) (2022) 4565–4575, https://doi.org/10.1007/s00603-022-02885-w

[34] Y. Gao, L. Hang, J. He, J. Chu, Mechanical behaviour of biocemented sands at various treatment levels and relative densities, Acta Geotech 14 (3) (2018) 697–707, https://doi.org/10.1007/s11440-018-0729-3

[35] M.G. Gomez, C.M. Anderson, C.M.R. Graddy, J.T. DeJong, D.C. Nelson, T.R. Ginn, Large-scale comparison of bioaugmentation and biostimulation approaches for biocementation of sands, J. Geotech. Geoenviron. Eng 143 (5) (2017), https://doi.org/10.1061/(asce)gt.1943-5606.0001640

[36] Gomez, M.G., Martinez, B.C., DeJong, J.T., Hunt, C.E., deVlaming, L.A., Major, D. W., Dworatzek, S.M., 2015. Field-scale bio-cementation tests to improve sands. Proceedings of the Institution of Civil Engineers - Ground Improvement. 168 (3), 206–216. http://dx.doi.org/10.1680/grim.13.00052.

[37] N. Guo, Y. Wang, X. Hui, Q. Zhao, Z. Zeng, S. Pan, Z. Guo, Y. Yin, T. Liu, Marine bacteria inhibit corrosion of steel via synergistic biomineralization, Journal of Materials Science & Technology 66 (2021) 82–90, https://doi.org/10.1016/j.jmst.2020.03.089
[38] Z. Guo, W. Wang, N. Guo, Z. Zeng, T. Liu, X. Wang, Molybdenum-mediated chemotaxis of Pseudoalteromonas lipolytica enhances biofilm-induced mineralization on low alloy steel surface, Corros. Sci. (2019) 159, https://doi.org/10.1016/j.corsci.2019.108123
[39] N. Hamdan, E. Kavazanjian, Enzyme-induced carbonate mineral precipitation for fugitive dust control, Géotechnique 66 (7) (2016) 546–555, https://doi.org/10.1680/jgeot.15.P.168
[40] L. Han, J. Li, Q. Xue, Z. Chen, Y. Zhou, C.S. Poon, Bacterial-induced mineralization (BIM) for soil solidification and heavy metal stabilization: a critical review, Sci. Total Environ. 746 (2020) 140967, https://doi.org/10.1016/j.scitotenv.2020.140967
[41] T. Hata, A.C. Saracho, S.K. Haigh, J. Yoneda, K. Yamamoto, Microbial-induced carbonate precipitation applicability with the methane hydrate-bearing layer microbe, J. Nat. Gas Sci. Eng. (2020) 81, https://doi.org/10.1016/j.jngse.2020.103490
[42] N. Hataf, A. Baharifard, Reducing soil permeability using microbial induced carbonate precipitation (MICP) method: a case study of shiraz landfill soil, Geomicrobiol. J. 37 (2) (2019) 147–158, https://doi.org/10.1080/01490451.2019.1678703
[43] J. He, J. Chu, Undrained responses of microbially desaturated sand under monotonic loading, J. Geotech. Geoenviron. Eng. 140 (5) (2014) 04014003, https://doi.org/10.1061/(ASCE)GT.1943-5606.0001082
[44] J. He, X. Chen, Q. Zhang, V. Achal, More effective immobilization of divalent lead than hexavalent chromium through carbonate mineralization by Staphylococcus epidermidis HJ2, Int. Biodeterior. Biodegrad. 140 (2019) 67–71, https://doi.org/10.1016/j.ibiod.2019.03.012
[45] J. Intarasoontron, W. Pungrasmi, P. Nuaklong, P. Jongvivatsakul, S. Likitlersuang, Comparing performances of MICP bacterial vegetative cell and microencapsulated bacterial spore methods on concrete crack healing, Constr. Build. Mater. (2021) 302, https://doi.org/10.1016/j.conbuildmat.2021.124227
[46] N. Jalilvand, A. Akhgar, H.A. Alikhani, H.A. Rahmani, F. Rejali, Removal of heavy metals zinc, lead, and cadmium by biomineralization of urease-producing bacteria isolated from iranian mine calcareous soils, J. Soil Sci. Plant Nutr. 20 (1) (2019) 206–219, https://doi.org/10.1007/s42729-019-00121-z
[47] N.J. Jiang, K. Soga, The applicability of microbially induced calcite precipitation (MICP) for internal erosion control in gravel–sand mixtures, Géotechnique 67 (1) (2017) 42–55, https://doi.org/10.1680/jgeot.15.P.182
[48] N.J. Jiang, R. Liu, Y.J. Du, Y.Z. Bi, Microbial induced carbonate precipitation for immobilizing Pb contaminants: Toxic effects on bacterial activity and immobilization efficiency, Sci. Total Environ. 672 (2019) 722–731, https://doi.org/10.1016/j.scitotenv.2019.03.294
[49] N.-J. Jiang, K. Soga, Erosional behavior of gravel-sand mixtures stabilized by microbially induced calcite precipitation (MICP, Soils Found 59 (3) (2019) 699–709, https://doi.org/10.1016/j.sandf.2019.02.003
[50] N.-J. Jiang, K. Soga, M. Kuo, Microbially induced carbonate precipitation for seepage-induced internal erosion control in sand–clay mixtures, J. Geotech. Geoenviron. Eng 143 (3) (2017), https://doi.org/10.1061/(asce)gt.1943-5606.0001559
[51] P. Jongvivatsakul, K. Janprasit, P. Nuaklong, W. Pungrasmi, S. Likitlersuang, Investigation of the crack healing performance in mortar using microbially induced calcium carbonate precipitation (MICP) method, Constr. Build. Mater. 212 (2019) 737–744, https://doi.org/10.1016/j.conbuildmat.2019.04.035
[52] C.-H. Kang, Y.-J. Kwon, J.-S. So, Bioremediation of heavy metals by using bacterial mixtures, Ecol. Eng. 89 (2016) 64–69, https://doi.org/10.1016/j.ecoleng.2016.01.023
[53] C.-H. Kang, S.J. Oh, Y. Shin, S.-H. Han, I.-H. Nam, J.-S. So, Bioremediation of lead by ureolytic bacteria isolated from soil at abandoned metal mines in South Korea, Ecol. Eng. 74 (2015) 402–407, https://doi.org/10.1016/j.ecoleng.2014.10.009
[54] M. Kanwal, R.A. Khushnood, F. Adnan, A.G. Wattoo, A. Jalil, Assessment of the MICP potential and corrosion inhibition of steel bars by biofilm forming bacteria in corrosive environment, Cem. Concr. Compos. (2023) 137, https://doi.org/10.1016/j.cemconcomp.2023.104937
[55] A. Karimian, M. Hassanlourad, Mechanical behaviour of MICP-treated silty sand, Bull. Eng. Geol. Environ. 81 (7) (2022), https://doi.org/10.1007/s10064-022-02780-2
[56] N. Kip, S. Jansen, M.F.A. Leite, M. de Hollander, M. Afanasyev, E.E. Kuramae, J.A.V. Veen, Methanogens predominate in natural corrosion protective layers on metal sheet piles, Sci. Rep. 7 (1) (2017) 11899, https://doi.org/10.1038/s41598-017-11244-7
[57] C.M. Kirkland, A. Thane, R. Hiebert, R. Hyatt, J. Kirksey, A.B. Cunningham, R. Gerlach, L. Spangler, A.J. Phillips, Addressing wellbore integrity and thief zone permeability using microbially-induced calcium carbonate precipitation (MICP): A field demonstration, Journal of Petroleum Science and Engineering (2020) 190, https://doi.org/10.1016/j.petrol.2020.107060
[58] O. Kolawole, I. Ispas, M. Kumar, J. Weber, B. Zhao, G. Zanoni, How can biogeomechanical alterations in shales impact caprock integrity and CO_2 storage? Fuel (2021) 291, https://doi.org/10.1016/j.fuel.2021.120149
[59] Konstantinou C., 2021. Hydraulic fracturing of artificially generated soft sandstones. University of Cambridge, (Doctoral thesis). https://doi.org/10.17863/CAM.64233.
[60] C. Konstantinou, G. Biscontin, Experimental investigation of the effects of porosity, hydraulic conductivity, strength, and flow rate on fluid flow in weakly cemented bio-treated sands, Hydrology 9 (11) (2022) 190, https://doi.org/10.3390/hydrology9110190
[61] C. Konstantinou, G. Biscontin, Soil enhancement via microbially induced calcite precipitation, Geotechnical Aspects of Underground Construction in Soft Ground, 2nd Edition, CRC Press, Cambridge, 2022, pp. 765–772, https://doi.org/10.1201/9781003355595
[62] C. Konstantinou, G. Biscontin, F. Logothetis, Tensile strength of artificially cemented sandstone generated via microbially induced carbonate precipitation, Materials 14 (2021) 4735, https://doi.org/10.3390/ma14164735
[63] Konstantinou, C., Biscontin, G., Papanastasiou, P., 2022. Interpretation of fluid injection experiments in poorly consolidated sands, In: 56th U.S. Rock Mechanics/Geomechanics Symposium. OnePetro, Santa Fe, New Mexico, USA, https://doi.org/10.56952/ARMA-2022–0632.
[64] C. Konstantinou, Y. Wang, G. Biscontin, A systematic study on the influence of grain characteristics on hydraulic and mechanical performance of MICP-treated porous media, Transp. Porous Media. (2023), https://doi.org/10.1007/s11242-023-01909-5
[65] C. Konstantinou, G. Biscontin, N.-J. Jiang, K. Soga, Application of microbially induced carbonate precipitation to form bio-cemented artificial sandstone, J. Rock Mech. Geotech. Eng. 13 (3) (2021) 579–592, https://doi.org/10.1016/j.jrmge.2021.01.010
[66] C. Konstantinou, Y. Wang, G. Biscontin, K. Soga, The role of bacterial urease activity on the uniformity of carbonate precipitation profiles of bio-treated coarse sand specimens, Sci Rep 11 (2021) 1–17, https://doi.org/10.1038/s41598-021-85712-6
[67] H.-l Kou, C.-z Wu, P.-p Ni, B.-A. Jang, Assessment of erosion resistance of biocemented sandy slope subjected to wave actions, Appl. Ocean Res. (2020) 105, https://doi.org/10.1016/j.apor.2020.102401
[68] S.E. Lambert, D.G. Randall, Manufacturing bio-bricks using microbial induced calcium carbonate precipitation and human urine, Water Res 160 (2019) 158–166, https://doi.org/10.1016/j.watres.2019.05.069
[69] M. Lee, M.G. Gomez, A.C.M. San Pablo, C.M. Kolbus, C.M.R. Graddy, J.T. DeJong, D.C. Nelson, Investigating ammonium by-product removal for ureolytic bio-cementation using meter-scale experiments, Sci. Rep. 9 (1) (2019) 18313, https://doi.org/10.1038/s41598-019-54666-1
[70] M. Li, K. Wen, Y. Li, L. Zhu, Impact of oxygen availability on microbially induced calcite precipitation (MICP) treatment, Geomicrobiol. J. 35 (1) (2017) 15–22, https://doi.org/10.1080/01490451.2017.1303553
[71] S. Li, C. Li, D. Yao, S. Wang, Feasibility of microbially induced carbonate precipitation and straw checkerboard barriers on desertification control and ecological restoration, Ecol. Eng. (2020) 152, https://doi.org/10.1016/j.ecoleng.2020.105883
[72] S. Li, Q. Qu, L. Li, K. Xia, Y. Li, T. Zhu, Bacillus cereus s-EPS as a dual bio-functional corrosion and scale inhibitor in artificial seawater, Water Res 166 (2019) 115094, https://doi.org/10.1016/j.watres.2019.115094
[73] H. Lin, M.T. Suleiman, D.G. Brown, E. Kavazanjian, Mechanical behavior of sands treated by microbially induced carbonate precipitation, J. Geotech. Geoenviron. Eng 142 (2) (2015), https://doi.org/10.1061/(asce)gt.1943-5606.0001383
[74] K.-W. Liu, N.-J. Jiang, J.-D. Qin, Y.-J. Wang, C.-S. Tang, X.-L. Han, An experimental study of mitigating coastal sand dune erosion by microbial- and enzymatic-induced carbonate precipitation, Acta Geotech 16 (2) (2020) 467–480, https://doi.org/10.1007/s11440-020-01046-z
[75] L. Liu, H. Liu, A.W. Stuedlein, T.M. Evans, Y. Xiao, Strength, stiffness, and microstructure characteristics of biocemented calcareous sand, Canadian Geotechnical Journal 56 (10) (2019) 1502–1513, https://doi.org/10.1139/cgj-2018-0007
[76] P. Liu, Y. Zhang, Q. Tang, S. Shi, Bioremediation of metal-contaminated soils by microbially-induced carbonate precipitation and its effects on ecotoxicity and long-term stability, Biochem. Eng. J. (2021) 166, https://doi.org/10.1016/j.bej.2020.107856
[77] S. Liu, R. Wang, J. Yu, X. Peng, Y. Cai, B. Tu, Effectiveness of the anti-erosion of an MICP coating on the surfaces of ancient clay roof tiles, Constr. Build. Mater. (2020) 243, https://doi.org/10.1016/j.conbuildmat.2020.118202
[78] T. Liu, Z. Guo, Z. Zeng, N. Guo, Y. Lei, T. Liu, S. Sun, X. Chang, Y. Yin, X. Wang, Marine bacteria provide lasting anticorrosion activity for steel via biofilm-induced mineralization, ACS Appl. Mater. Interfaces. 10 (46) (2018) 40317–40327, https://doi.org/10.1021/acsami.8b14991
[79] A. Mahawish, A. Bouazza, W.P. Gates, Unconfined compressive strength and visualization of the microstructure of coarse sand subjected to different biocementation levels, J. Geotech. Geoenviron. Eng. 145 (8) (2019), https://doi.org/10.1061/(asce)gt.1943-5606.0002066
[80] A. Martinez, L. Huang, M.G. Gomez, Thermal conductivity of MICP-treated sands at varying degrees of saturation, Géotech. Lett. 9 (1) (2019) 15–21, https://doi.org/10.1680/jgele.18.00126
[81] B.C. Martinez, J.T. DeJong, T.R. Ginn, B.M. Montoya, T.H. Barkouki, C. Hunt, B. Tanyu, D. Major, Experimental optimization of microbial-induced carbonate precipitation for soil improvement, J. Geotech. Geoenviron. Eng. 139 (4) (2013) 587–598, https://doi.org/10.1061/(asce)gt.1943-5606.0000787
[82] T. Marzin, B. Desvages, A. Creppy, L. Lépine, A. Esnault-Filet, H. Auradou, Using microfluidic set-up to determine the adsorption rate of sporosarcina pasteurii bacteria on sandstone, Transp. Porous Media. 132 (2) (2020) 283–297, https://doi.org/10.1007/s11242-020-01391-3
[83] H. Meng, Y. Gao, J. He, Y. Qi, L. Hang, Microbially induced carbonate precipitation for wind erosion control of desert soil: Field-scale tests, Geoderma (2021) 383, https://doi.org/10.1016/j.geoderma.2020.114723
[84] B.M. Montoya, J.T. DeJong, Stress-strain behavior of sands cemented by

microbially inudced carbonate precipitation, J. Geotech. Geoenviron. Eng. 141 (6) (2015) 04015019, https://doi.org/10.1061/(ASCE)GT.1943-5606
[85] B.M. Montoya, J.T. Dejong, R.W. Boulanger, Dynamic response of liquefiable sand improved by microbial-induced calcite precipitation, Géotechnique 63 (4) (2013) 302–312, https://doi.org/10.1680/geot.SIP13.P.019
[86] S.-W. Moon, G. Vinoth, S. Subramanian, J. Kim, T. Ku, Effect of fine particles on strength and stiffness of cement treated sand, Granular Matter 22 (1) (2019), https://doi.org/10.1007/s10035-019-0975-6
[87] A.J. Mugwar, M.J. Harbottle, Toxicity effects on metal sequestration by microbially-induced carbonate precipitation, J. Hazard. Mater. 314 (2016) 237–248, https://doi.org/10.1016/j.jhazmat.2016.04.039
[88] D. Mujah, L. Cheng, M.A. Shahin, Microstructural and geomechanical study on biocemented sand for optimization of MICP process, J. Mater. Civ. Eng 31 (4) (2019), https://doi.org/10.1061/(asce)mt.1943-5533.0002660
[89] W. Mwandira, K. Nakashima, S. Kawasaki, Bioremediation of lead-contaminated mine waste by Pararhodobacter sp. based on the microbially induced calcium carbonate precipitation technique and its effects on strength of coarse and fine grained sand, Ecol. Eng. 109 (2017) 57–64, https://doi.org/10.1016/j.ecoleng.2017.09.011
[90] D. de Oliveira, E.J. Horn, D.G. Randall, Copper mine tailings valorization using microbial induced calcium carbonate precipitation, J. Environ. Manage 298 (2021) 113440, https://doi.org/10.1016/j.jenvman.2021.113440
[91] L.A. van Paassen, R. Ghose, T.J.M. van der Linden, W.R.L. van der Star, M.C.M. van Loosdrecht, Quantifying biomediated ground improvement by ureolysis: large-scale biogrout experiment, J. Geotech. Geoenviron. Eng. 136 (2010) 1721–1728, https://doi.org/10.1061/(ASCE)GT.1943-5606.0000382
[92] D. Peng, S. Qiao, Y. Luo, H. Ma, L. Zhang, S. Hou, B. Wu, H. Xu, Performance of microbial induced carbonate precipitation for immobilizing Cd in water and soil, J. Hazard. Mater. 400 (2020) 123116, https://doi.org/10.1016/j.jhazmat.2020.123116
[93] J. Peng, Z. Liu, Influence of temperature on microbially induced calcium carbonate precipitation for soil treatment, PLoS One 14 (6) (2019) e0218396, https://doi.org/10.1371/journal.pone.0218396
[94] S. Peng, H. Di, L. Fan, W. Fan, L. Qin, Factors affecting permeability reduction of MICP for fractured rock, Front. Earth Sci (2020) 8, https://doi.org/10.3389/feart.2020.00217
[95] A.J. Phillips, E. Troyer, R. Hiebert, C. Kirkland, R. Gerlach, A.B. Cunningham, L. Spangler, J. Kirksey, W. Rowe, R. Esposito, Enhancing wellbore cement integrity with microbially induced calcite precipitation (MICP): a field scale demonstration, Journal of Petroleum Science and Engineering 171 (2018) 1141–1148, https://doi.org/10.1016/j.petrol.2018.08.012
[96] A.J. Phillips, A.B. Cunningham, R. Gerlach, R. Hiebert, C. Hwang, B.P. Lomans, J. Westrich, C. Mantilla, J. Kirksey, R. Esposito, L. Spangler, Fracture sealing with microbially-induced calcium carbonate precipitation: a field study, Environ. Sci. Technol. 50 (7) (2016) 4111–4117, https://doi.org/10.1021/acs.est.5b05559
[97] A.A. Qabany, K. Soga, Effect of chemical treatment used in MICP on engineering properties of cemented soils, Géotechnique 63 (4) (2013) 331–339, https://doi.org/10.1680/geot.SIP13.P.022
[98] C. Qian, T. Zheng, X. Zhang, Y. Su, Application of microbial self-healing concrete: case study, Constr. Build. Mater. (2021) 290, https://doi.org/10.1016/j.conbuildmat.2021.123226
[99] X. Qian, C. Fang, M. Huang, V. Achal, Characterization of fungal-mediated carbonate precipitation in the biomineralization of chromate and lead from an aqueous solution and soil, J. Cleaner Prod. 164 (2017) 198–208, https://doi.org/10.1016/j.jclepro.2017.06.195
[100] S. Qiao, G. Zeng, X. Wang, C. Dai, M. Sheng, Q. Chen, F. Xu, H. Xu, Multiple heavy metals immobilization based on microbially induced carbonate precipitation by ureolytic bacteria and the precipitation patterns exploration, Chemosphere (2021) 274, https://doi.org/10.1016/j.chemosphere.2021.129661
[101] K. Rowshanbakht, M. Khamehchiyan, R.H. Sajedi, M.R. Nikudel, Effect of injected bacterial suspension volume and relative density on carbonate precipitation resulting from microbial treatment, Ecol. Eng. 89 (2016) 49–55, https://doi.org/10.1016/j.ecoleng.2016.01.010
[102] E. Salifu, E. MacLachlan, K.R. Iyer, C.W. Knapp, A. Tarantino, Application of microbially induced calcite precipitation in erosion mitigation and stabilisation of sandy soil foreshore slopes: a preliminary investigation, Eng. Geol. 201 (2016) 96–105, https://doi.org/10.1016/j.enggeo.2015.12.027
[103] A.C.M. San Pablo, M. Lee, C.M.R. Graddy, C.M. Kolbus, M. Khan, A. Zamani, N. Martin, C. Acuff, J.T. DeJong, M.G. Gomez, D.C. Nelson, Meter-scale biocementation experiments to advance process control and reduce impacts: examining spatial control, ammonium by-product removal, and chemical reductions, J. Geotech. Geoenviron. Eng 146 (11) (2020), https://doi.org/10.1061/(asce)gt.1943-5606.0002377
[104] M.A. Shahin, K. Jamieson, L. Cheng, Microbial-induced carbonate precipitation for coastal erosion mitigation of sandy slopes, Géotech. Lett. 10 (2) (2020) 211–215, https://doi.org/10.1680/jgele.19.00093
[105] M. Sharma, N. Satyam, K.R. Reddy, Large-scale spatial characterization and liquefaction resistance of sand by hybrid bacteria induced biocementation, Eng. Geol. (2022) 302, https://doi.org/10.1016/j.enggeo.2022.106635
[106] G. Shi, J. Qi, Y. Wang, S. Liu, Experimental study on the prevention of coal mine dust with biological dust suppressant, Powder Technol 391 (2021) 162–172, https://doi.org/10.1016/j.powtec.2021.05.096
[107] M. Simatupang, M. Okamura, Liquefaction resistance of sand remediated with carbonate precipitation at different degrees of saturation during curing, Soils Found 57 (4) (2017) 619–631, https://doi.org/10.1016/j.sandf.2017.04.003
[108] M. Simatupang, M. Okamura, K. Hayashi, H. Yasuhara, Small-strain shear modulus and liquefaction resistance of sand with carbonate precipitation, Soil Dyn. Earthquake Eng 115 (2018) 710–718, https://doi.org/10.1016/j.soildyn.2018.09.027
[109] M.G. Sohail, Z.A. Disi, N. Zouari, N.A. Nuaimi, R. Kahraman, B. Gencturk, D.F. Rodrigues, Y. Yildirim, Bio self-healing concrete using MICP by an indigenous Bacillus cereus strain isolated from Qatari soil, Constr. Build. Mater. (2022) 328, https://doi.org/10.1016/j.conbuildmat.2022.126943
[110] N.W. Soon, L.M. Lee, T.C. Khun, H.S. Ling, Factors affecting improvement in engineering properties of residual soil through microbial-induced calcite precipitation, J. Geotech. Geoenviron. Eng 140 (5) (2014), https://doi.org/10.1061/(asce)gt.1943-5606.0001089
[111] V. Stabnikov, V. Ivanov, J. Chu, Sealing of sand using spraying and percolating biogrouts for the construction of model aquaculture pond in arid desert, Int. Aquat. Res,. 8 (3) (2016) 207–216, https://doi.org/10.1007/s40071-016-0136-z
[112] X. Sun, L. Miao, R. Chen, H. Wang, L. Wu, J. Xia, Liquefaction resistance of biocemented loess soil, J. Geotech. Geoenviron. Eng 147 (11) (2021), https://doi.org/10.1061/(asce)gt.1943-5606.0002638
[113] S. Tang, X. Chang, M. Li, T. Ge, S. Niu, D. Wang, Y. Jiang, S. Sun, Fabrication of calcium carbonate coated-stainless steel mesh for efficient oil-water separation via bacterially induced biomineralization technique, Chem. Eng. J. (2021) 405, https://doi.org/10.1016/j.cej.2020.126597
[114] S. Tang, S. Sun, T. Liu, M. Li, Y. Jiang, D. Wang, N. Guo, Z. Guo, X. Chang, Bionic engineering-induced formation of hierarchical structured minerals with superwetting surfaces for oil-water separation, J. Membr. Sci. (2023) 669, https://doi.org/10.1016/j.memsci.2022.121261
[115] D. Terzis, L. Laloui, Cell-free soil bio-cementation with strength, dilatancy and fabric characterization, Acta Geotech 14 (3) (2019) 639–656, https://doi.org/10.1007/s11440-019-00764-3
[116] D. Terzis, L. Laloui, S. Dornberger, R. Harran, In A Full-Scale Application of Slope Stabilization via Calcite Bio-Mineralization Followed by Long-Term GIS Surveillance, Geo-Congress on Biogeotechnics, Minneapolis, MN, Minneapolis, MN, 2020.
[117] D.J. Tobler, J.M. Minto, G. El Mountassir, R.J. Lunn, V.R. Phoenix, Microscale analysis of fractured rock sealed with microbially induced CaCO3 precipitation: influence on hydraulic and mechanical performance, Water Resour. Res. 54 (10) (2018) 8295–8308, https://doi.org/10.1029/2018wr023032
[118] S. Venuleo, L. Laloui, D. Terzis, T. Hueckel, M. Hassan, Microbially induced calcite precipitation effect on soil thermal conductivity, Géotechnique Letters 6 (1) (2016) 39–44, https://doi.org/10.1680/jgele.15.00125
[119] X. Wang, J. Xu, Z. Wang, W. Yao, Use of recycled concrete aggregates as carriers for self-healing of concrete cracks by bacteria with high urease activity, Constr. Build. Mater. (2022) 337, https://doi.org/10.1016/j.conbuildmat.2022.127581
[120] Y. Wang, K. Soga, J.T. DeJong, A.J. Kabla, Microscale visualization of microbial-induced calcium carbonate precipitation processes, J. Geotech. Geoenviron. Eng 145 (9) (2019), https://doi.org/10.1061/(asce)gt.1943-5606.0002079
[121] Y. Wang, K. Soga, J.T. Dejong, A.J. Kabla, A microfluidic chip and its use in characterising the particle-scale behaviour of microbial-induced calcium carbonate precipitation (MICP), Géotechnique 69 (12) (2019) 1086–1094, https://doi.org/10.1680/jgeot.18.P.031
[122] Y. Wang, K. Soga, J.T. DeJong, A.J. Kabla, Effects of bacterial density on growth rate and characteristics of microbial-induced CaCO3 precipitates: particle-scale experimental study, J. Geotech. Geoenviron. Eng 147 (6) (2021), https://doi.org/10.1061/(asce)gt.1943-5606.0002509
[123] Wang, Y.Z., Soga, K., Jiang, N.J., Microbial induced carbonate precipitation (MICP): the case for microscale perspective. In 19th International Conference on Soil Mechanics and Geotechnical Engineering, Seoul, South Korea, 2017.
[124] Z. Wang, N. Zhang, Y. Jin, Q. Li, J. Xu, Application of microbially induced calcium carbonate precipitation (MICP) in sand embankments for scouring/erosion control, Marine Georesour. Geotechnol. 39 (12) (2020) 1459–1471, https://doi.org/10.1080/1064119x.2020.1850949
[125] Z. Wang, N. Zhang, J. Ding, Q. Li, J. Xu, Thermal conductivity of sands treated with microbially induced calcite precipitation (MICP) and model prediction, Int. J. Heat Mass Transfer. (2020) 147, https://doi.org/10.1016/j.ijheatmasstransfer.2019.118899
[126] V.S. Whiffin, L.A. van Paassen, M.P. Harkes, Microbial carbonate precipitation as a soil improvement technique, Geomicrobiol. J. 24 (5) (2007) 417–423, https://doi.org/10.1080/01490450701436505
[127] C. Wu, J. Chu, S. Wu, Y. Hong, 3D characterization of microbially induced carbonate precipitation in rock fracture and the resulted permeability reduction, Eng. Geol. 249 (2019) 23–30, https://doi.org/10.1016/j.enggeo.2018.12.017
[128] S. Wu, B. Li, J. Chu, Stress-dilatancy behavior of MICP-treated sand, Int. J. Geomech 21 (3) (2021), https://doi.org/10.1061/(asce)gm.1943-5622.0001923
[129] P. Xiao, H. Liu, Y. Xiao, A.W. Stuedlein, T.M. Evans, Liquefaction resistance of biocemented calcareous sand, Soil Dyn. Earthquake Eng 107 (2018) 9–19, https://doi.org/10.1016/j.soildyn.2018.01.008
[130] Y. Xiao, Y. Wang, C.S. Desai, X. Jiang, H. Liu, Strength and deformation responses of biocemented sands using a temperature-controlled method, Int. J. Geomech 19 (11) (2019), https://doi.org/10.1061/(asce)gm.1943-5622.0001497
[131] Y. Xiao, X. He, A.W. Stuedlein, J. Chu, T. Matthew Evans, L.A. van Paassen, Crystal growth of MICP through microfluidic chip tests, J. Geotech. Geoenviron. Eng 148 (5) (2022), https://doi.org/10.1061/(asce)gt.1943-5606.0002756
[132] Y. Xiao, X. He, W. Wu, A.W. Stuedlein, T.M. Evans, J. Chu, H. Liu, L.A. van Paassen, H. Wu, Kinetic biomineralization through microfluidic chip tests, Acta Geotech 16 (10) (2021) 3229–3237, https://doi.org/10.1007/s11440-021-01205-w
[133] J. Yang, X. Pan, C. Zhao, S. Mou, V. Achal, F.A. Al-Misned, M.G. Mortuza, G.M. Gadd, Bioimmobilization of heavy metals in acidic copper mine tailings soil,

Geomicrobiol. J. 33 (3–4) (2016) 261–266, https://doi.org/10.1080/01490451.2015.1068889
[134] Z. Yang, X. Cheng, A performance study of high-strength microbial mortar produced by low pressure grouting for the reinforcement of deteriorated masonry structures, Construction and Building Materials 41 (2013) 505–515, https://doi.org/10.1016/j.conbuildmat.2012.12.055
[135] T. Yin, H. Lin, Y. Dong, B. Li, Y. He, C. Liu, X. Chen, A novel constructed carbonate-mineralized functional bacterial consortium for high-efficiency cadmium biomineralization, J. Hazard. Mater. 401 (2021) 123269, https://doi.org/10.1016/j.jhazmat.2020.123269
[136] X. Yu, H. Rong, Seawater based MICP cements two/one-phase cemented sand blocks, Appl. Ocean Res. (2022) 118, https://doi.org/10.1016/j.apor.2021.102972
[137] H. Yuan, Q. Zhang, X. Hu, M. Wu, Y. Zhao, Y. Feng, D. Shen, Application of zeolite as a bacterial carrier in the self-healing of cement mortar cracks, Constr. Build. Mater. (2022) 331, https://doi.org/10.1016/j.conbuildmat.2022.127324
[138] A. Zamani, B.M. Montoya, Undrained monotonic shear response of MICP-treated silty sands, J. Geotech. Geoenviron. Eng 144 (6) (2018), https://doi.org/10.1061/(asce)gt.1943-5606.0001861
[139] A. Zamani, B.M. Montoya, Undrained cyclic response of silty sands improved by microbial induced calcium carbonate precipitation, Soil Dyn. Earthquake Eng 120 (2019) 436–448, https://doi.org/10.1016/j.soildyn.2019.01.010
[140] A. Zamani, B.M. Montoya, M.A. Gabr, Investigating challenges of in situ delivery of microbial-induced calcium carbonate precipitation (MICP) in fine-grain sands and silty sand, Can. Geotech. J. 56 (12) (2019) 1889–1900, https://doi.org/10.1139/cgj-2018-0551
[141] Y. Zeng, Z. Chen, Y. Du, Q. Lyu, Z. Yang, Y. Liu, Z. Yan, Microbiologically induced calcite precipitation technology for mineralizing lead and cadmium in landfill leachate, J. Environ. Manag. 296 (2021) 113199, https://doi.org/10.1016/j.jenvman.2021.113199
[142] C. Zhang, T. Shi, J. Liu, Z. He, H. Thomas, H. Dong, B. Rinkevich, Y. Wang, J.H. Hyun, M. Weinbauer, C. Lopez-Abbate, Q. Tu, S. Xie, Y. Yamashita, P. Tishchenko, Q. Chen, R. Zhang, N. Jiao, Eco-engineering approaches for ocean negative carbon emission, Sci Bull 67 (24) (2022) 2564–2573, https://doi.org/10.1016/j.scib.2022.11.016
[143] M. Zhang, L. Zhao, G.K. Li, C. Zhu, S. Dong, Z. Li, C. Tang, J. Ji, J. Chen, Microbially induced magnesium carbonate precipitation and its potential application in combating desertification, Geomicrobiol. J. 38 (6) (2021) 549–560, https://doi.org/10.1080/01490451.2021.1900461
[144] C. Zhao, Q. Fu, W. Song, D. Zhang, J. Ahati, X. Pan, F.A. Al-Misned, M.G. Mortuza, Calcifying cyanobacterium (Nostoc calcicola) reactor as a promising way to remove cadmium from water, Ecol. Eng. 81 (2015) 107–114, https://doi.org/10.1016/j.ecoleng.2015.04.012
[145] Y. Zhao, L. Peng, W. Zeng, Cs Poon, Z. Lu, Improvement in properties of concrete with modified RCA by microbial induced carbonate precipitation, Cem. Concr. Compos. (2021) 124, https://doi.org/10.1016/j.cemconcomp.2021.104251
[146] M. Zhong, B. Liu, L. Zhang, J. Wang, J. Chen, J. Li, Y. Liu, L. Ming, Experimental study on microbial induced calcium carbonate precipitation to enhance reservoir recovery, Iran. J. Biotechnol. 20 (1) (2022) e3024, https://doi.org/10.30498/ijb.2021.279942.3024
[147] S.M.A. Zomorodian, H. Ghaffari, B.C. O'Kelly, Stabilisation of crustal sand layer using biocementation technique for wind erosion control, Aeolian Res. 40 (2019) 34–41, https://doi.org/10.1016/j.aeolia.2019.06.001